

THE
NMR
NEWSLETTER

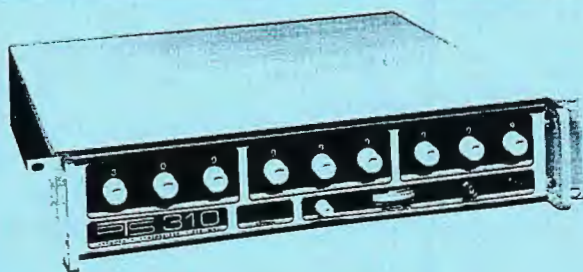
No. 503
August 2000

| | | |
|--------------------------------------------------------------------------------------------------------------------------------------------------------------------------------------------------------------|------------------------------------------|-----------|
| Numerical Diagonal Suppression in COSY | Delaglio, F., Wu, J., and Bax, A. | 2 |
| Fitting Chemical Exchange Spectra | Bain, A. D. | 7 |
| Magnet Pressure Regulation: Take a NAP van Os, J., Janssen, H., Vuister, G., and Kentgens, A. | | 11 |
| Compressed Air Supplies for NMR Spectrometers: Update Fishbein, K. W., and Spencer, R. G. S. | | 15 |
| Dynamics of Hindered 5,6-Diarylacenaphthenes | Hawkes, G. E., and Nasser, R. | 19 |
| $^2J, ^3J$ -HMBC: Unequivocal Differentiation of $^2J_{CH}$ from $^3J_{CH}$ Long-Range Correlations to Protonated Carbons . Martin, G. E., Russell, D. J., Hadden, C. E., and Krishnamurthy, V. V. | | 23 |
| Positions Available | Stockman, B. J. | 25 |
| Field of Dreams, XI. "Relaxation Agent Warning" | Shaffer, K. | 31 |
| Position Available | Gmeiner, W. H. | 32 |

A monthly collection of informal private letters from laboratories involved with NMR spectroscopy. Information contained herein is solely for the use of the reader. Quotation of material from the Newsletter is *not* permitted, except by direct arrangement with the author of the letter, in which case the material quoted *must* be referred to as a "Private Communication". Results, findings, and opinions appearing in the Newsletter are solely the responsibility of the author(s). Reference to The NMR Newsletter or its previous names in the open literature is strictly forbidden.

These restrictions and policies apply equally to both the actual Newsletter recipient/participants and to all others who are allowed access to the Newsletter issues. Strict adherence to this policy is considered essential to the successful continuation of the Newsletter as an informal medium for the exchange of NMR-related information.

| | Frequency Range | Resolution | Switching Time | Phase-Continuous Switching | Rack-Mount Cabinet Dim. ¹ | Remote-Control Interface | Price Example ² |
|-----------------------------|---------------------------------|------------------------------|----------------|----------------------------|--------------------------------------|-------------------------------|--------------------------------------------------------------------------|
| PTS 040 | .1-40 MHz | optional .1 Hz to 100 KHz | 1-20 μ s | optional | 5¼"H×19"W | BCD (std) or GPIB (opt) | \$5,330.00 (1 Hz resol., OCXO freq. std.) |
| PTS 120 | 90-120 MHz | optional .1 Hz to 100 KHz | 1-20 μ s | optional | 5¼"H×19"W | BCD (std) or GPIB (opt) | \$5,330.00 (1 Hz resol., OCXO freq. std.) |
| PTS 160 | .1-160 MHz | optional .1 Hz to 100 KHz | 1-20 μ s | optional | 5¼"H×19"W | BCD (std) or GPIB (opt) | \$6,495.00 (1 Hz resol., OCXO freq. std.) |
| PTS 250 | 1-250 MHz | optional .1 Hz to 100 KHz | 1-20 μ s | optional | 5¼"H×19"W | BCD (std) or GPIB (opt) | \$7,440.00 (1 Hz resol., OCXO freq. std.) |
| Type 1 PTS 310 Type 2 | .1-310 MHz | .1 Hz | 1-20 μ s | standard | 3½"H×19"W | BCD (std) or GPIB (opt) | 1 Hz resol., OCXO: \$6,425.00 1 Hz resol., OCXO: \$5,850.00 |
| PTS 500 | 1-500 MHz | optional .1 Hz to 100 KHz | 1-20 μ s | optional | 5¼"H×19"W | BCD (std) or GPIB (opt) | \$8,720.00 (1 Hz resol., OCXO freq. std.) |
| PTS 620 | 1-620 MHz | optional .1 Hz to 100 KHz | 1-20 μ s | optional | 5¼"H×19"W | BCD (std) or GPIB (opt) | \$9,625.00 (1 Hz resol., OCXO freq. std.) |
| PTS 1000 | 0.1-1000 MHz | optional .1 Hz to 100 KHz | 5-10 μ s | optional | 5¼"H×19"W | BCD (std) or GPIB (opt) | \$11,830.00 (1 Hz resol., OCXO freq. std.) |
| PTS 3200 | 1-3200 MHz | 1 Hz | 1-20 μ s | optional | 5¼"H×19"W | BCD (std) or GPIB (opt) | \$14,850.00 (1 Hz resol., OCXO freq. std.) |
| PTS x10 | user specified 10 MHz decade | 1 Hz | 1-5 μ s | standard | 3½"H×19"W | BCD (std) or GPIB (opt) | \$3,000.00 (1 Hz resol., OCXO freq. std.) |
| PTS D310 | two channels .1-310 MHz | .1 Hz | 1-20 μ s | standard | 5¼"H×19"W | BCD (std) or GPIB (opt) | \$8,560.00 (.1 Hz resol., OCXO freq. std.) |
| PTS D620 | two channels 1-620 MHz | .1 Hz/.2 Hz | 1-20 μ s | standard | 5¼"H×19"W | BCD (std) or GPIB (opt) | \$13,240.00 (.1 Hz/.2 Hz resol., OCXO freq. std.) |



1 Bench cabinets are 17" wide.

2 Prices are U.S. only and include Manual and Remote (BCD) Control; PTS 3200 Digital Front Panel.

PTS CAN SUPPLY OEM-TYPE SYNTHESIZERS FOR ALL LEADING NMR-SPECTROMETER PRODUCTS.

PROGRAMMED TEST SOURCES, INC.

P.O. Box 517, 9 Beaver Brook Rd., Littleton, MA 01460 Tel: 978-486-3400 Fax: 978-486-4495

http://www.programmedtest.com • e-mail: sales@programmedtest.com

| THE NMR NEWSLETTER | | NO. 503, AUGUST 2000 | | AUTHOR INDEX | |
|-------------------------|----|------------------------------|----|---------------------------|----|
| Bain, A. D. | 7 | Hadden, C. E. | 23 | Martin, G. E. | 23 |
| Bax, A. | 2 | Hawkes, G. E. | 19 | Nasser, R. | 19 |
| Delaglio, F. | 2 | Janssen, H. | 11 | van Os, J. | 11 |
| Fishbein, K. W. | 15 | Kentgens, A. | 11 | Russell, D. J. | 23 |
| Gmeiner, W. H. | 32 | Krishnamurthy, V. V. | 23 | Shaffer, K. | 31 |
| | | | | Spencer, R. G. S. | 15 |
| | | | | Stockman, B. J. | 25 |
| | | | | Vuister, G. | 11 |
| | | | | Wu, J. | 2 |

| THE NMR NEWSLETTER | | NO. 503, AUGUST 2000 | | ADVERTISER INDEX | |
|--------------------------------------|----|-------------------------------|--------------------|------------------|--|
| Advanced Chemistry Development, Inc. | 17 | JEOL | outside back cover | | |
| AMT | 13 | Programmed Test Sources, Inc. | inside front cover | | |
| Avanti Polar Lipids, Inc. | 21 | Varian, Inc. | 5 | | |
| Bruker Instruments, Inc. | 9 | Voltronics Corporation. | 25 | | |

SPONSORS OF THE NMR NEWSLETTER

Abbott Laboratories
 Advanced Chemistry Development, Inc.
 Aldrich Chemical Company, Inc.
 Amgen, Inc.
 AMT
 Anasazi Instruments, Inc.
 AstraZeneca
 Avanti Polar Lipids, Inc.
 Bruker Instruments, Inc.
 Bristol-Myers Squibb Company
 Cambridge Isotope Laboratories
 Cryomag Services, Inc.
 The Dow Chemical Company

E. I. du Pont de Nemours & Company
 Isotec, Inc.
 JEOL (U.S.A.) Inc., Analytical Instruments Division
 The Lilly Research Laboratories, Eli Lilly & Company
 Merck Research Laboratories
 Nalorac Corporation
 Pharmacia & Upjohn, Inc.
 Programmed Test Sources, Inc.
 SINTEF Unimed MR Center, Trondheim, Norway
 Tecmag
 Unilever Research
 Union Carbide Corporation
 Varian, Inc.

FORTHCOMING NMR MEETINGS

XIX International Conference on Mag. Res. in Biological Systems, Florence, Italy, **August 20-25, 2000**. Contact: Profs. Ivano Bentini or Lucia Banci, Chem. Dept., Univ. of Florence, Via G. Capponi 7, I-50121, Florence, Italy; Phone: +39-055-2757600; Email: icmrbs@lrm.fi.cnr.it; Fax: +39-055-2757555; <http://www.lrm.fi.cnr.it/icmrbs.html>.

NMR: Drug Discovery and Design Conference – Post-Genomic Analysis, McLean, Virginia, **October 24-26, 2000**. Contact: Mary Chitty, Cambridge Healthtech Institute, mchitty@healthtech.com; Fax 617-630-1325.

NMR Spectroscopy of Biofluids and Tissues, Imperial College, London, England, **November 13-17, 2000**. Contact: Hersha Mistry, Centre for Continuing Education, Imperial College, 526 Sherfield Building, Exhibition Road, London, SW7 2AZ, UK. Tel: +44 (0)20 7594 6884; Fax: +44 (0)20 7594 6883; Email: h.mistry@ic.ac.uk; <http://www.ad.ic.ac.uk/cpd/nmr.htm>

42nd ENC (Experimental NMR Conference), Rosen Plaza Hotel, Orlando, Florida, **March 11-16, 2001**; Arthur G. Palmer, Chair: Agp6@columbia.edu; Contact: ENC, 1201 Don Diego Avenue, Santa Fe, NM 87505; (505) 989-4573; Fax: (505) 989-1073; E-mail: enc@enc-conference.org; Web: enc-conference.org

Gordon Research Conference on Magnetic Resonance, **June 17-22, 2001**, Roger Williams University, Bristol, Rhode Island (note the new, improved location !!!). Contacts: Rob Tycko, Chair, 301-402-8272, tycko@helix.nih.gov, and Kurt Zilm, Vice-Chair, kurt.zilm@yale.edu. Site description and application information available at <http://www.grc.uri.edu>.

Royal Society of Chemistry: 15th International Meeting on NMR Spectroscopy, Durham, England, **week of July 8-13, 2001**; Contact: Mrs. Paula Whelan, The Royal Society of Chemistry, Burlington House, London W1V 0BN, England; +44 0171 440 3316; Email: conferences@rsc.org

ISMAR 2001, Jerusalem, Israel, **August 19-24, 2001**; See <http://www.tau.ac.il/chemistry/ISMAR.html>.

Additional listings of meetings, etc., are invited.

Numerical Diagonal Suppression in COSYNational Institute of Diabetes and
Digestive and Kidney Diseases
Bethesda, Maryland 20892

July 4, 2000

(received 7/7/2000)

Dear Barry,

Under the gentle guidance and encouragement of Ad Bax, we've been revisiting the problem of measuring proton-proton couplings from traditional COSY spectra. Of course, the problem in COSY spectra is well known: In both frequency dimensions, the diagonal is 90° out of phase relative to the cross peaks. So, when phasing the cross peaks to be absorptive, the tails from the dispersive diagonal peaks obscure many of the nearby cross peaks (see top panel of Figure). A long, long time ago, Luciano Mueller suggested an elegant way of subtracting the diagonal by conducting a COSY experiment without a mixing pulse (1). Alternatively, such a no-mixing pulse "COSY" spectrum can be generated from a single FID (2). Unfortunately, in Ad's soupy samples, which besides our little molecules contain liquid crystal such as bicelles or phages, this trick does not work so well. Instead, we therefore went back and tried to attenuate the diagonal signals numerically. We've had good results using a scheme that combines frequency shifting with methods usually used for solvent signal subtraction, such as the time-domain convolution method (3) and time-domain polynomial subtraction (4). As you know, these solvent subtraction methods are designed to suppress low-frequency signals, i.e. those at the center of the spectrum. Therefore, if we temporarily shift columns of a 2D spectrum in such a way that the diagonal signal is moved to the center, these low-frequency suppression methods can also be used for diagonal suppression. This means we need to apply an amount of shifting that varies according to the position of the diagonal signal in any given column (vector). Since frequency shifting can be achieved by a first-order phase correction in the time domain, the diagonal suppression steps can all be carried out in the t_1 time domain. In practice, after the t_2 Fourier transformation and absorptive phasing, the frequency shifting, diagonal subtraction, and frequency unshifting are applied to the t_1 vectors of the 2D data matrix.

We've implemented this scheme using facilities of our software system NMRPipe. This may be especially apropos, since interestingly (if you find obscure NMR software history interesting) the very first application of our pipeline-based software was implementation of a diagonal zeroing method by Mitsu Ikura and Istvan Pelczer, a close relative of the current scheme. In any event, a complete description of NMRPipe in its current form, including details on how to decipher processing schemes such as the ones here, can be found at: <http://spin.niddk.nih.gov/bax/software>.

(1) L. Mueller, *J. Magn. Reson.* **72**, 191 (1987).

(2) D. Marion and A. Bax, *J. Magn. Reson.* **80**, 528-533 (1988).

(3) Marion D., Ikura, M., and Bax, A., *J. Magn. Reson.* **84**, 425-430 (1989).

(4) Callaghan, P.T., MacKay, A.L., Pauls, K.P., Soderman, O., and Bloom, M., *J. Magn. Reson.* **56**, 101-109 (1984).

An example UNIX processing pipeline script for our 2D COSY processing is shown below. In the scheme, the directly-detected dimension is processed as usual, but with the signals of the first t_1 increment phased absorptively after the first FT. Then, each t_1 vector in the indirect dimension is shifted via phase correction so that its diagonal signal becomes on-resonance, a "solvent" filter is applied by subtracting a best-fit 4th or 5th order polynomial, and the vector is shifted back again. The solvent filter methods sometimes distort intensities at the head and tail of the time-domain data, leading to baseline curvature near the region of signal suppression in the spectrum. So in this case, since the signals of interest are sine-modulated, the leading points of the time-domain data can be attenuated with a suitable window without affecting the cross peak signals. Here, we used a custom roll-off function with a cosine-squared form. After these diagonal suppression steps, the t_1 vectors are then processed as usual, and finally, the direct dimension is rephased to dispersive mode. The script is annotated to describe the processing steps, with the functions applied to the indirect dimension given in bold:

```
nmrPipe -in test.fid \
| nmrPipe -fn SP -off 0.5 -pow 2 -end 0.95 -c 0.5 \
| nmrPipe -fn ZF -size 2048 \
| nmrPipe -fn FT -verb \
| nmrPipe -fn PS -p0 138.7 -p1 18.1 -di \
| nmrPipe -fn TP \
| nmrPipe -fn MAC -macro diagShift.M \
| nmrPipe -fn POLY -time \
| nmrPipe -fn MAC -macro diagUnShift.M \
| nmrPipe -fn MAC -macro csr.M -var wide 10 \
| nmrPipe -fn SP -off 0.5 -pow 2 -end 0.95 -c 1.0 \
| nmrPipe -fn ZF -size 2048 \
| nmrPipe -fn FT -verb \
| nmrPipe -fn PS -p0 -110 -p1 220 -di \
| nmrPipe -fn POLY -auto \
| nmrPipe -fn TP \
| nmrPipe -fn POLY -auto \
| nmrPipe -fn PS -p0 90 -ht -di \
-out test.ft2 -verb -ov
```

Read FID
Window, 1st Point Scale
Zero Fill
Fourier Transform
F2 Phase Correction
2D Transpose
Shift Diagonal to Center
Polynomial Solvent Filter
Shift Diagonal Back
Attenuate Head of FID
Window
Zero Fill
Fourier Transform
F1 Phase Correction
Auto Baseline Correction
2D Transpose
Auto Baseline Correction
Rephase F2 to Dispersive
Write Spectrum

We decided to implement the shifting operations using the macro interpreter facility of NMRPipe, which allows custom functions to be included in processing schemes without the need to compile new versions of the software. The macro language is a subset of the C programming language, augmented with a number of vector processing functions. The shifting macro `diagShift.M` is shown below; it is invoked once for each t_1 vector in the interferogram. The macro language provides many automatically defined variables that describe the current data. In this case, the variables `xSize` and `ySize` give the number of points in t_1 and f_2 respectively, and `yLoc` gives the index number of the t_1 vector being processed, in the range of 1 to `ySize`. The variables `rdata` and `idata` are arrays containing the real and imaginary parts of the current vector. Finally, `phase()` is a vector processing function which applies a zero and first order correction as given in degrees:

```
xMid = 1 + xSize/2;
yMid = 1 + ySize/2;

slope = (1 - xMid)/(yMid - 1);
offset = -slope*yMid;
shift = slope*yLoc + offset;

p0 = 0.0;
p1 = -360.0*shift;

(void) phase( rdata, idata, xSize, p0, p1 );
```

The cosine-squared roll-off function was also implemented as a macro, `csr.M`, shown here. This function multiplies the data by a function that increases from zero to one over the first several points in the data, and leaves the remainder of the data unchanged. The number of points attenuated is specified by the variable `wide`, which is taken from the command-line of the processing script:

```
for( i = 0; i < wide; i++ )
{
  c = cos( 0.5*PI*i/wide );
  w = 1.0 - c*c;

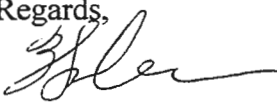
  rdata[i] *= w;
  idata[i] *= w;
}
```

On the right, an example result is shown for a diagonal region in a 2D COSY of a DNA sample, spanning 2.96 to 1.44 ppm. The topmost contour plot shows the result of conventional processing, which predictably is dominated by the diagonal, making the crosspeaks very hard to see or measure. The central contour plot shows the same data, as processed with the diagonal suppression scheme. The crosspeaks here are easily seen, and in this case even those close to the diagonal can be quantified. The contour plot at bottom shows the diagonal signal alone, as generated by taking the difference between the original and diagonal suppressed data, then rephasing both dimensions to absorptive mode. In this case, the diagonal is well isolated and undistorted, and can also be quantified. All three plots have been drawn with the same contour parameters.

We hope this may play some part in generating renewed interest in COSY spectra of biomolecules.

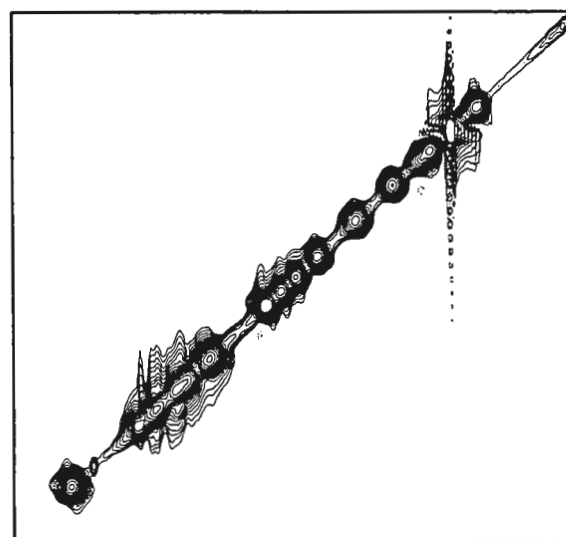
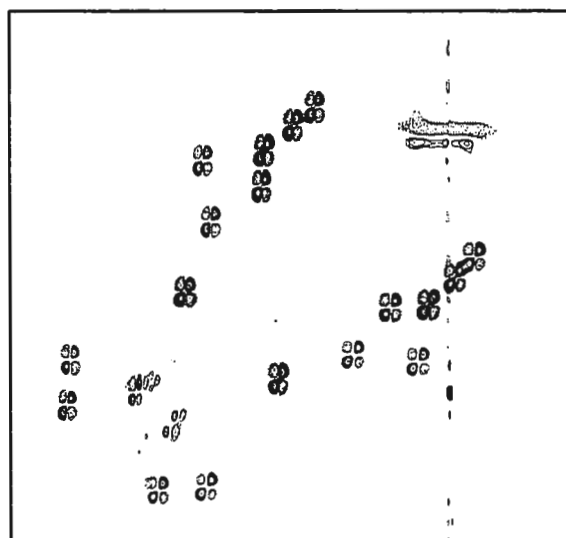
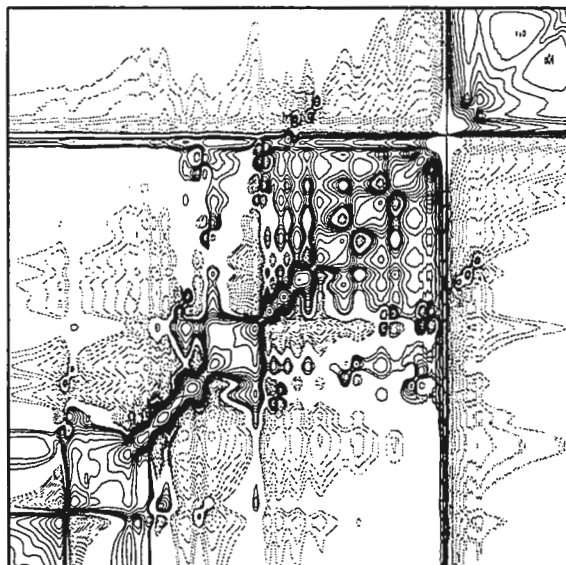
Many Cheerful Regards,


Frank Delaglio

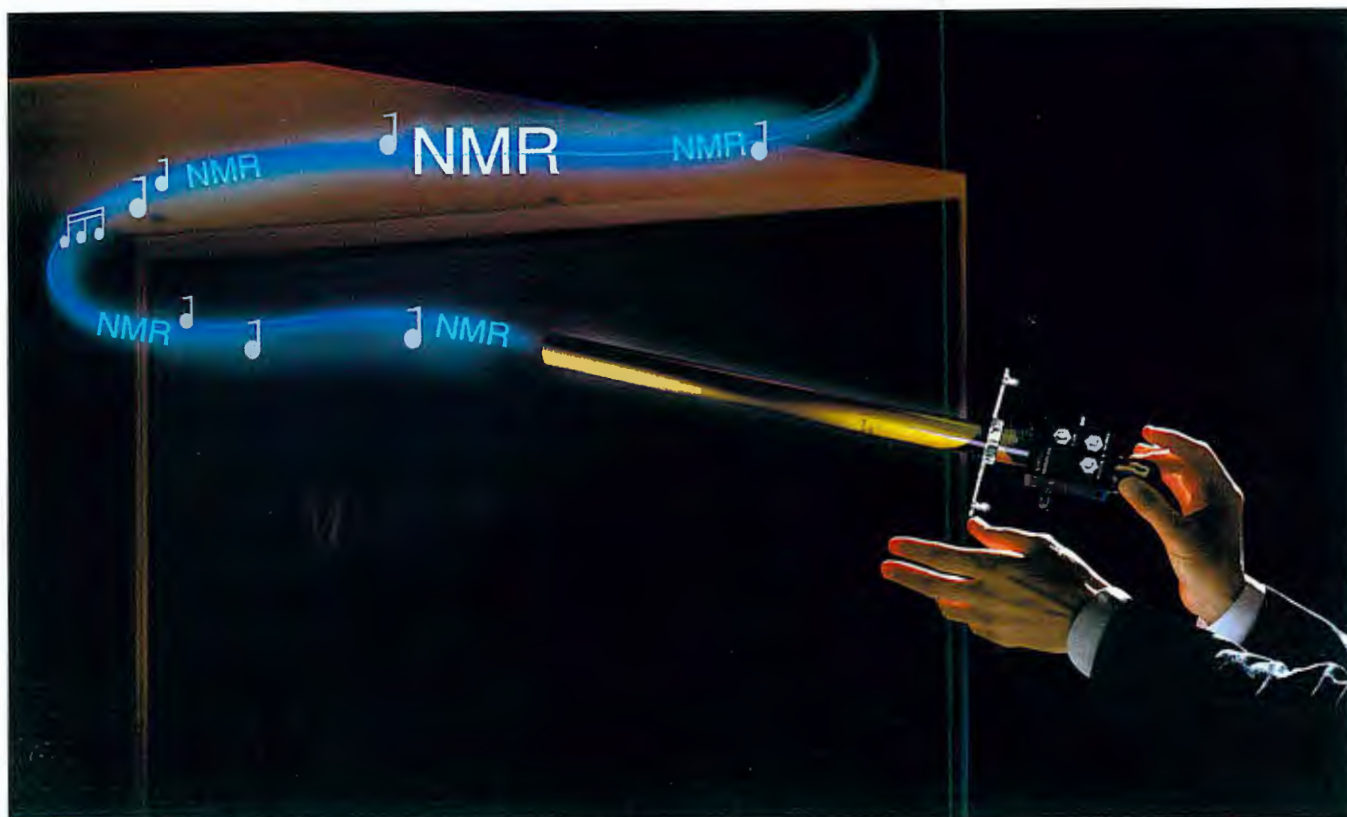

Justin Wu

as prepared with the earnest benedictions of,

Ad Bax



Perfectly Tuned for Every Performance.



Varian's Mercury and new ATB Probe move NMR at a faster tempo.

When you're conducting NMR experiments on samples in different solvents, an out-of-tune probe can ruin your whole performance.

Our innovative Automation Triple Broadband (ATB) Probe's unique circuit design eliminates tuning for each sample, saving costly analysis time. This is accomplished without adjusting ANY parts of the probe. The result: an impressive improvement in reliability.

There is no need to worry about changing solvents when using the

ATB Probe. It delivers less than a 5% change in the PW90 from DMSO- d_6 samples to $CDCl_3$ samples. As we say around Varian, it's the "Always Tuned Beautifully" probe.

Combine the ATB Probe with the powerful, economical Mercury 300 MHz system and today's most exciting NMR experiments are just a double click away.

Call or visit our website to experience truly remarkable NMR performance.

1.800.356.4437
650.424.4890

www.varianinc.com/nmr/mercury



VARIAN

MERCURY and the Automation Triple Broadband Probe: Automation done right!

Varian has the intelligent solution: the 300 MHz **MERCURY** and the Automation Triple Broadband (ATB) $^1\text{H}/^{19}\text{F}/\text{X}$ probe. Varian's exciting new Automation Triple Broadband probe sets a new standard for automated NMR data analysis excellence by eliminating one of the most persistent problems in unattended NMR analysis—sensitivity losses between samples in different solvents.

No probe tuning required for samples in solvents ranging from DMSO...



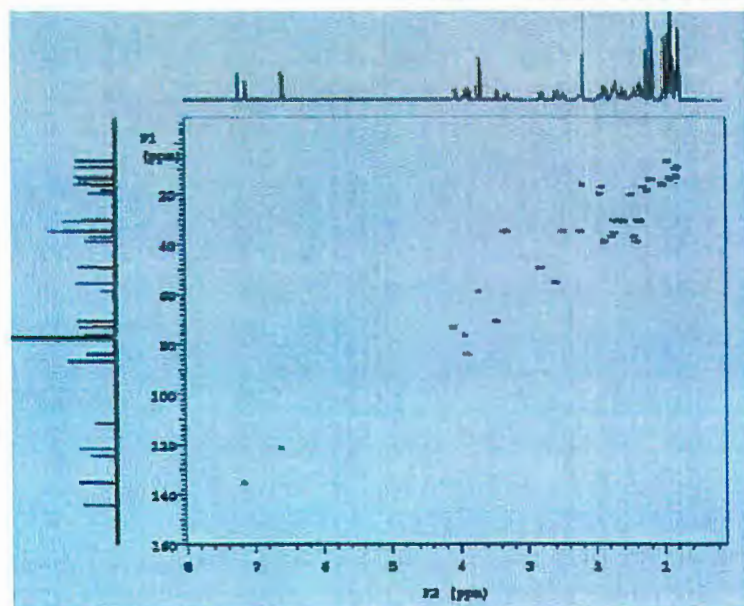
^{13}C nutation profile of DMSO in $\text{DMSO}-d_6$...

...to Benzene...



^{13}C nutation profile of $^{13}\text{CH}_3\text{I}$ in $\text{Benzene}-d_6$...

...to Chloroform!



HSQC of lasalocid-A in CDCl_3 , acquired with no tuning of the sample.

Combine the new ATB probe with the powerful, economical **MERCURY** system, and you can access today's most exciting direct and indirect detection NMR experiments with just a mouse-click. Just use **MERCURY**'s intuitive push-button interface and automated system calibration and be certain in obtaining the very best sensitivity from your NMR experiment.

1.800.356.4437
650.424.4890
www.varianinc.com/nmr/mercury



VARIAN



Department of
Chemistry

1280 Main Street West
Hamilton, Ontario, Canada
L8S 4M1

Phone: 905.525.9140
Ext. 23490
Fax: 905.522.2509

June 16, 2000 (received 6/26/2000)

Dr. B.L. Shapiro
The NMR Newsletter
966 Elsinore Court
Palo Alto, CA
U.S.A. 94303-3410

Fitting Chemical Exchange Spectra

Dear Barry,

We are still messing around with chemical exchange. The simulation of lineshapes for both coupled and uncoupled systems in liquids is now under control, with the programs MEX and MEXICO. We have also recently been working with solids. Floquet theory, combined with some clever ways to diagonalize matrices, turns out to be a good way to use to simulate the effect of exchange on spinning sideband patterns, but that's another story.

We want to make the programs iterative, so that we don't have to sit in front of the computer, constantly tinkering with rates and other parameters. This means that we need to teach the computer to explore the X^2 surface - the hypersurface which shows the misfit between calculated and observed spectra, as a function of the parameters. If we understand the general shape of the surface, then the fitting procedure becomes clearer.

The simplest case is two-site equally-populated exchange - the classic Gutowsky and Holm case. If k is the exchange rate, and the chemical shift difference is given by 2δ (the lines in the absence of exchange appear at $\pm\delta$), then the lineshape, as a function of frequency, ω , can be written as in equation [1].

$$\text{lineshape} = f(\omega) = \frac{4k^2\delta^2}{(\omega^2 - \delta^2)^2 + 4k^2\omega^2} \quad [1]$$

If the digitized, observed spectrum is given by $s(\omega)$, where ω is represented by the digital points, then the X^2 surface is given by equation [2].

$$X^2 = \sum_{\text{points}} (s(\omega) - f(\omega))^2 \quad [2]$$

Note that since $f(\omega)$ depends on k and δ , then X^2 is also a function of those two variables. If we assume the fit is reasonably good, then the difference $(s(\omega) - f(\omega))$ is like a differential, $df(\omega)$. When we expand the differential into its partial derivative components, equation [2] becomes [3].

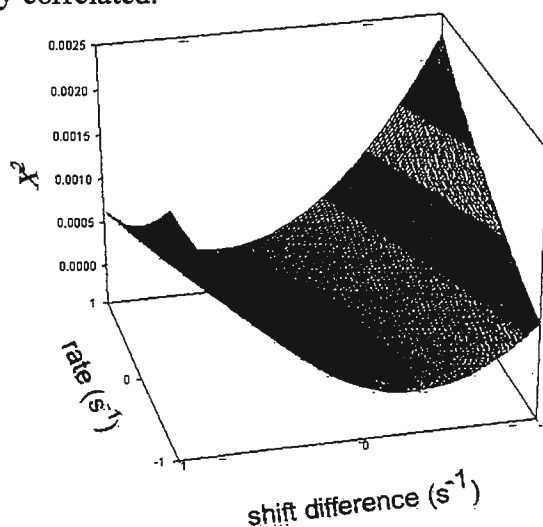
$$\begin{aligned}
X^2 &= \sum_{\text{points}} (s(\omega) - f(\omega))^2 \\
&= \sum_{\text{points}} (df(\omega))^2 \\
&= \sum_{\text{points}} \left(\frac{\partial f}{\partial k} dk + \frac{\partial f}{\partial \delta} d\delta \right)^2
\end{aligned}
\tag{3}$$

If we now expand this sum, we get equation [4].

$$\begin{aligned}
X^2 &= \sum_{\text{points}} \left(\frac{\partial f}{\partial k} dk + \frac{\partial f}{\partial \delta} d\delta \right)^2 \\
&= (dk)^2 \sum_{\text{points}} \left(\frac{\partial f}{\partial k} \right)^2 + 2(dk)(d\delta) \sum_{\text{points}} \left(\frac{\partial f}{\partial k} \right) \left(\frac{\partial f}{\partial \delta} \right) + (d\delta)^2 \sum_{\text{points}} \left(\frac{\partial f}{\partial \delta} \right)^2
\end{aligned}
\tag{4}$$

This is a quadratic form, which we can plot as a function of the offsets from optimum of the rate and the shift difference. For the case of the rate being half of the coalescence rate, the plot of equation [4] is shown in the figure.

We know that in slow exchange, we can determine both the rate and the shift difference. If these were completely independent, the contours in the figure would be circular. The strong elliptical character indicates that even at this rate, there is a strong correlation between the rate and the shift difference. In fast exchange, of course, we can determine only the ratio, but the plot shows that even before coalescence, the two parameters are strongly correlated.

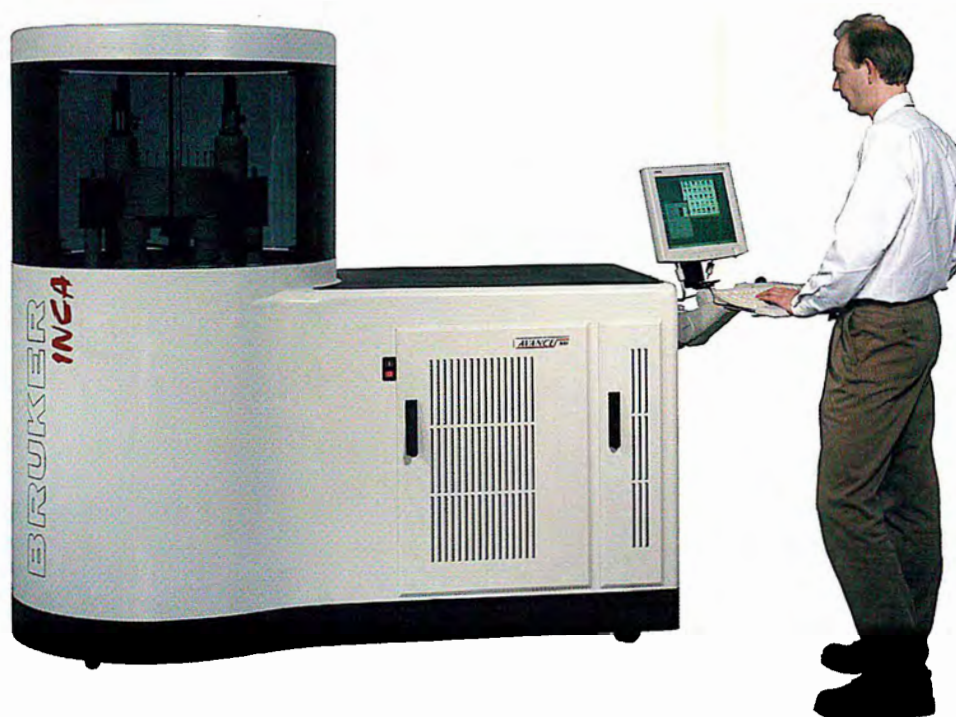


Yours truly,

Alex D. Bain
bain@mcmaster.ca



NMR goes plug-and-play.



INCA™

The new paradigm in NMR chemical analysis:

**Integrated
NMR
Chemical
Analyzer**

- *The power of FT-NMR for chemical analysis, at-line process analysis, in-vitro diagnosis*
- *A safe, non-intimidating analyzer for "non-NMR spectroscopists"*
- *Ergonomic design in a small footprint*
- *Magnet, electronics and PC-control in one rugged, movable unit*
- *UltraShield magnet (300/400 MHz) keeps the 5 Gauss line within the enclosure*



INCA™ - Integrated NMR Chemical Analyzer

The INCA is designed for use by technicians who need the analytical power of a modern FT-NMR for value-added applications, but have limited space and support for a traditional NMR spectroscopy lab.

Value-Added Applications

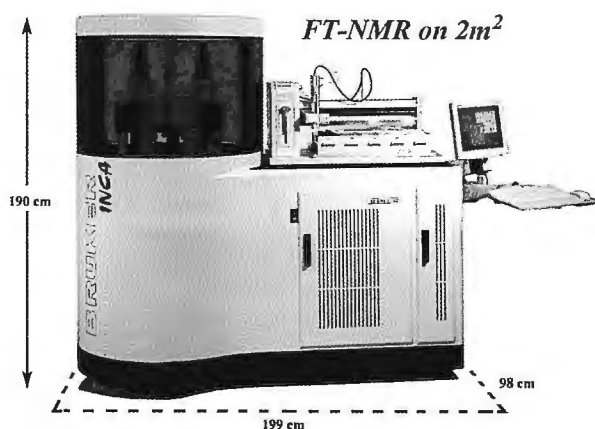
The INCA is an easy-to-use, and robust solution for routine chemical analysis, at-line process analysis, and in-vitro diagnostics. The Windows NT operating system and the programmable user interface enable the INCA to be operated in a routine fashion by anyone using a touch screen. While the technicians may only have access to one (or a few) dedicated protocols, the INCA system can be modified by an expert spectroscopist to create revenue generating protocols and other new experiments.

Safety

The INCA, available at 300 and 400 MHz, radically reduces the footprint required for NMR. External connections are limited to a single power cord and an air supply. The use of the Bruker UltraShield magnet keeps the 5 Gauss field line within the enclosure and alleviates concerns for operators not used to the safety aspects of an NMR lab.

Expansion Possibilities

The INCA can be equipped with a number of different accessories. Add SampleTrack, our LIMS software for data tracking, and one of our many sample handling systems for complete automation from data submission to output of results. Samples can be delivered in conventional NMR tubes and placed into our NMR CASE™ autosampler. Or use one of our many flow probes together with the Gilson Autosampler for high throughput applications. Post processing of the data with Bruker AMIX software gives easy access to multi-variate analysis. The INCA can be customized to meet your exact specifications for varied sample delivery and measurement!



INCA Specifications:

| | |
|-------------------------------|----------------------------|
| Height | 1900 mm (6'2") |
| Length | 1990 mm (6'6") |
| Depth | 980 mm (3'3") |
| Magnet | 300/400 MHz UltraShield |
| Computer | Pentium PC |
| OS | Windows NT |
| Display | LCD Flat Panel Touchscreen |
| RF Specifications | same as AVANCE Series |
| NMR Methods | full AVANCE pulse library |
| VT | optional |
| B₀ gradient | optional |
| Probes | Application-specific |

Australia : BRUKER (AUSTRALIA) PTY. LTD., ALEXANDRIA, NSW 2015, Phone: (61) 2 95506422
 Belgium : BRUKER BELGIUM S.A./N.V., 1140 BRUXELLES / BRUSSEL, Phone: (32) 2 7267626
 Canada : BRUKER CANADA LTD., MILTON, Ont. L9T 1Y6, Phone: (1) 905 8764641
 BRUKER CANADA LTD., SIDNEY, B.C. V8L 5Y8, Phone: (1) 250 6561622
 France : BRUKER S.A., 67166 WISSEMBOURG / Cedex, Phone: (33) 3 88 736800
 Germany : BRUKER ANALYTIK GMBH, 76287 RHEINSTETTEN, Phone: (49) 721 51610
 BRUKER ANALYTIK GMBH 76189 KARLSRUHE, Phone: (49) 721 95280
 Great Britain : BRUKER UK LIMITED, COVENTRY CV4 9GH, Phone: (44) 1203 855200
 India : BRUKER INDIA SCIENTIFIC PVT. LTD., MUMBAI - 400 063, Phone: (91) 22 849 0060
 Israel : BRUKER SCIENTIFIC ISRAEL LTD., REHOVOT 76 123, Phone: (972) 8 9409660
 Italy : BRUKER ITALIANA SRL, 20133 MILANO, Phone: (39) 2 70636370
 Japan : BRUKER JAPAN CO. LTD., IBARAKI 305-0051, Phone: (81) 298 521234
 BRUKER JAPAN CO. LTD., OSAKA 564-0051, Phone: (81) 6 3397008
 Mexico : BRUKER MEXICANA, S. A. de C. V., MEXICO, D.F. CP 14210, Phone: (52) 5 6305747
 Netherlands : BRUKER NEDERLAND NV, 1530 AB WORMER, Phone: (31) 75 6285251
 P.R. China : BRUKER INSTRUMENTS LTD., BEIJING 100081, Phone: (86) 10 6847-2015
 Spain : BRUKER ESPANOLA, S. A., MADRID, Phone: (34) 1 6559013
 Sweden : BRUKER SCANDINAVIA AB, 187 66 TÄBY, Phone: (46) 8 4463630
 Switzerland : BRUKER AG, 8117 FÄLLANDEN, Phone: (41) 1 8259111
 Thailand : BRUKER SOUTH EAST ASIA, BANGKOK 10400, Phone: (66) 2 6426900
 United States : BRUKER INSTRUMENTS, INC., BILLERICA, MA. 01821-3991, Phone: (1) 978 6679580
 Regional offices in FREMONT, CA. 94539, Phone: (1) 510 6834300,
 WESTMONT, IL. 60532, Phone: (1) 630 3236194, NEWARK, DE. 19810, Phone: (1) 302 8369066
 THE WOODLANDS, TX 77381, Phone: (1) 2812922447

For complete details contact your
local Bruker sales representative.

We'd like to hear from you.

www.bruker.com/nmr



Dr. B.L. Shapiro
The NMR Newsletter
966 Elsinore Court
Palo Alto, CA 94303
U.S.A.

(received 7/12/2000)
Nijmegen, June 30, 1999

Magnet pressure regulation; take a NAP.

Variations in atmospheric pressure hamper optimal use of modern high-field high-resolution NMR spectrometers. This is caused by the fact that pressure variations cause variations in the boiling temperature of He and thus induce instabilities in the magnet. As a consequence, absolute pressure regulators for the helium Dewar have become a standard part of high-field magnets that are newly installed.

So far the available pressure regulation-units are electronic devices using an absolute pressure sensor and a regulated helium valve. The valves in use are of the "normally open"-type to minimize dangerous situations in case of a power failure. In general, however, there is always the risk of a malfunction in such an electronic device, which, if not potentially dangerous, can be a nuisance if they cause degradation of the obtained spectra. Furthermore, there is the matter of cost if one wants to install these devices on older magnets.

We have developed a simple alternative for the electronic pressure regulators, based on physical principles only. The idea is very straightforward as will be described below. Our first prototype built a few weeks ago was tested on an Oxford 600 widebore magnet and performed according to our expectations. We would like to call it the Nijmegen Absolute Pressure (NAP)-regulation, it certainly avoids losing precious sleep worrying over pressure regulation. The basic operation is explained by means of the drawing in Figure 1.

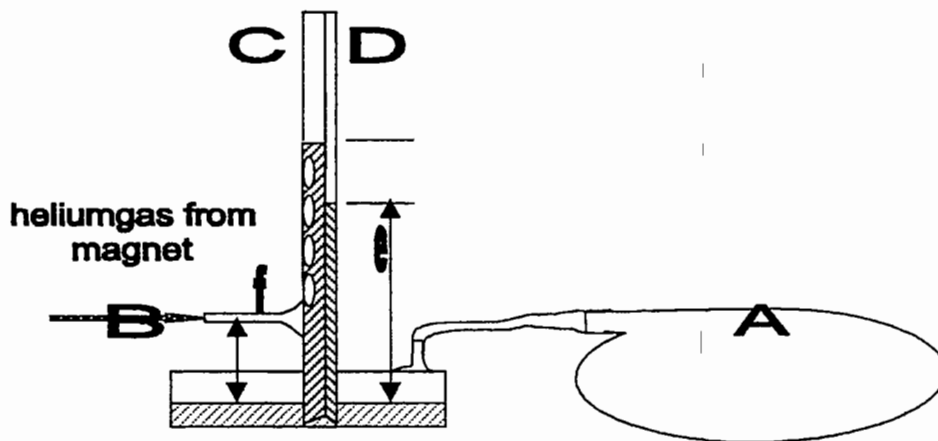


Fig. 1: Schematic setup of the "Nijmegen Double Barrel"

The device consists of two vessels, denoted A and B and two pipes C and D. The vessels A and B are connected as shown. Vessel B is partly filled with oil whereas a pressure above normal atmospheric pressure is applied to vessel A. As a result the oil rises in the pipes C and D due to the difference in pressure in vessel A and the room pressure.

In the test setup we have chosen a large volume of 100 liters for vessel A filled with nitrogen to a reference pressure of 1042 mbar. Vessel B is partly filled with oil ($\rho=0.83 \text{ gr/cm}^3$). The cross section of pipes C (0.95 cm^2) and D (0.28 cm^2) is small compared to that of vessel B which has a surface area of 250 cm^2 . The inlet for the helium gas is $\sim 10 \text{ cm}$ (f) above the oil level in B. It can easily be seen that the outlet pressure of the



magnet is going to be $1042 - 0.83 \cdot 10 = 1034$ mbar. This is exactly what we measure. We do not observe any noticeable variation of the magnet pressure with varying atmospheric pressure. We do observe a dependence of ambient temperature and magnet pressure.

This is fully understandable if we look at the gas laws. A simple calculation shows that atmospheric pressure variations are scaled down by a factor 0.005 (pipe area / area vessel B) at the magnet outlet if we assume the volume of A large enough so that its pressure remains constant. To give a practical example: an increase of 10 mbar in atmospheric pressure will cause the height "e" to change $10 / 0.83 = 12$ cm in first approximation. The volume decrease in A will only be $12 \cdot (0.95 + 0.28) = 14.75$ cm³ giving rise to a negligible pressure rise of $(14.75 / 100000) \cdot 1042 = 0.15$ mbar. The level in B is changing by only $14.75 / 250 = -0.059$ cm, corresponding to a pressure change of -0.05 mbar. Normal changes in atmospheric pressure thus cause negligible pressure variations at the magnet outlet.

The sensitivity for temperature variations is a different matter, as these variations will cause a variation in the pressure of vessel A; an increase in temperature of 1 degree will cause the pressure in A to go up by 3.5 mbar. As the temperature in NMR labs is regulated anyhow we consider this a minor drawback.

The level in pipe C will be higher than that in D because the average specific gravity of the oil-helium mixture in C is less than that of the "pure" oil in D. Also the oil level in C will be diffuse because of the helium bubbles. This does not influence the static pressure at height "f" above the oil surface, meaning the regulated pressure can be exactly determined in pipe D, without influencing the regulating power of the device. The relative difference in height between the two levels in C and D is indicative for the evaporation rate of the magnet. This way the device, alternatively named the "Double Barrel" serves two purposes. It maintains an absolute pressure in the helium Dewar and it is indicative for its evaporation rate.

The first advantage over an electronic device is the absence of electronic circuits. The worst thing that can happen to the setup, a leak any of the components, results in a safe situation where the magnet boils off at atmospheric pressure. The second one is the costs that are involved, which is a fraction of the costs of commercially available units. A third advantage is its visibility; one look at the device indicates strange changes in pressure and gives a good indication of the evaporation rate of the Dewar.

The disadvantages of the device are the temperature dependence and the volume of the reference vessel A. The temperature dependence of the device is about 3.5 mbar per Kelvin. This is not a major problem because if the temperature stability in the magnet area is poor, the magnet will be unstable anyhow. The second disadvantage, that of the volume in A, can be overcome by doing some arithmetic. Our prototype is based upon neglecting pressure variations in A by choosing a large volume. As we already saw, an increase in atmospheric pressure causes an increase of the pressure in A and as a result a slight decrease in the magnet pressure. We can put this to our advantage. A proper choice of the volume of A leads to a cancellation of external pressure variations at the magnet outlet. Calculations show that with our current setup we would need volumes between 2.5 to 5 liters, making the device small enough to attach it as a whole to the magnet. When the color of the "reminder" gives rise to it, we will probably report on this "small NAP".

Best wishes,

Jan van Os

Hans Janssen

Geerten Vuister

Arno Kentgens

Your Source for RF Amplifiers



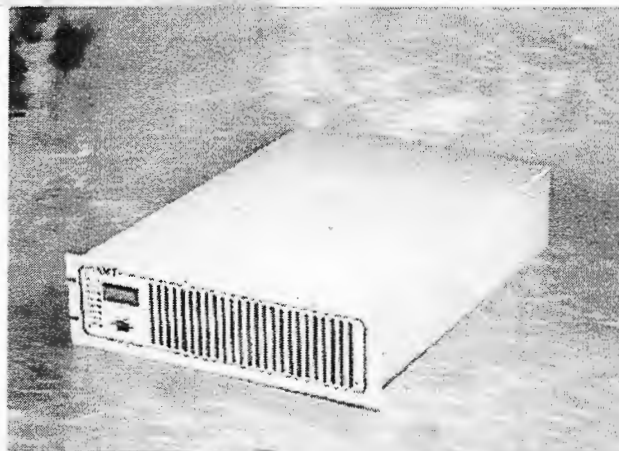
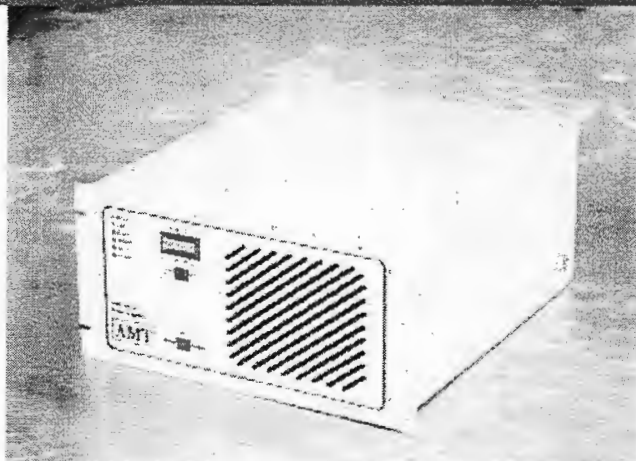
ISO 9001
CERTIFIED

2570 E. Cerritos Avenue
Anaheim, CA 92806

Phone: 714-456-0777

Fax: 714-456-0780

www.amtinc.com



SCIENTIFIC PRODUCTS

AMT's scientific products are used extensively in Nuclear Magnetic Resonance (NMR) systems. These amplifiers cover the frequency ranges of 6 MHz to 500 MHz, with power levels as high as 2.0 kW peak power at 10% duty cycle.

MEDICAL PRODUCTS

AMT's medical products are employed in Magnetic Resonance Imaging (MRI) systems. These amplifiers cover the frequency range from 10 MHz to 200 MHz with power levels as high as 12 kW peak power at 10% duty cycle.

Your Source for RF Amplifiers

AMT IS:

- ⇒ LEADING SUPPLIER OF AMPLIFIERS
- ⇒ CUSTOMER SENSITIVE
- ⇒ ISO 9001 CERTIFIED

AMT AMPLIFIERS ARE:

- ⇒ PULSED OR CW MODE OPERATION
- ⇒ HIGHLY RELIABLE
- ⇒ SOLID STATE
- ⇒ COST EFFECTIVE



ISO 9001
CERTIFIED

2570 E. Cerritos Avenue
Anaheim, CA 92806

Phone: 714-456-0777
Fax: 714-456-0780
www.amtinc.com



DEPARTMENT OF HEALTH & HUMAN SERVICES

Public Health Service

Dr. B.L. Shapiro
The NMR Newsletter
966 Elsinore Court
Palo Alto, CA 94303

National Institutes of Health
National Institute on Aging
Gerontology Research Center
5600 Nathan Shock Drive
Baltimore, MD 21224

(received 6/26/2000)
June 17, 2000

Compressed Air Supplies for NMR Spectrometers: An Update

Dear Barry,

Since we described a quiet, self-contained compressed air supply for NMR spectrometers based on a Powerex rotary scroll air compressor in our 1995 letter (*The NMR Newsletter*, No. 442), we have received many inquiries about this system. In the six years since that system was installed, there have been several significant developments which we would like to pass on to your readers.

First and most importantly, we wish to emphasize the danger presented by using a glass bottle to collect the condensed water from the compressor, tank, and air driers. Originally, we had used a polyethylene carboy for condensate collection but this container soon split open at the seams due to mechanical fatigue from numerous cycles of compression and depressurization. We then switched to using a 25 liter glass bottle, which worked without incident for more than four years before exploding early one morning, spraying glass shrapnel into every corner of the NMR room! Fortunately, there were no injuries or property damage, but we now use a bottle completely wrapped in duct tape and sealed inside a thick-walled steel barrel filled with absorbent material. Because the level of condensate in the collector is no longer directly visible, we use a rod attached to a cork floating on the liquid surface to determine when the bottle should be emptied. Based on this experience, we strongly advise anyone installing a compressed air system to discharge the condensate into a sink or drain pipe if possible and to carefully consider how the pressure built up by each discharge cycle will be vented.

Another major point of failure in the original design was the pneumatic condensate drain valves. These valves were designed to automatically open when the condensate collected caused a certain preset pressure drop and were attractive because they required no electrical supply or timers. Unfortunately, all of the pneumatic valves, both on the refrigerated and desiccant driers, eventually became clogged with scale and dirt and subsequently failed. We replaced them with solenoid-activated valves controlled by an electronic timer. These proved much more reliable, but were vulnerable to sticking in the open position, causing a loss of air pressure and sometimes a compressor shutdown due to excessive duty cycle and overheating. At present, we are installing electrically-operated ball valves, which promise to be yet more resistant to clogging.

After six years of operation, the compressor itself began to overheat regularly and we found that the rotary scroll compressor head had seized, probably due to a failure of the tip seals. These tip seals are an important potential point of failure in the scroll compressor design and they must be replaced by a factory-trained technician every 10,000 hours of operation. The compressor failure may also have been associated with the earlier failure of a gate-type check valve attached to the compressor's built-in tank. When this valve failed, the compressor began to run *backwards* for several seconds each time the motor shut off until, eventually, the gate flap within the valve broke off and was sucked into the scroll assembly. After this incident, we replaced the gate-type check valve with a spring-loaded ball valve, which has proved highly reliable. Ultimately, we decided to

replace the entire compressor, and so we reviewed the currently-available compressor technology and came to the conclusion that the rotary scroll compressor is still the only viable option if one must put the compressor in an inhabited area, especially the NMR room itself. Consequently, we ordered a replacement compressor of the same type, except with a 5 HP capacity to decrease the duty cycle and therefore, we hope, prolong the compressor's lifetime. We should emphasize that it is the Balston air drier which really uses up most of the compressor's capacity, and the 3 HP unit was marginally too small to accommodate this demand.

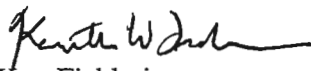
When installing a new rotary scroll compressor, we have found that it is crucial to measure the actual voltages supplied to the unit and to compare them to the motor's voltage settings. Because the rotary scroll compressor is completely enclosed on all sides, it is especially vulnerable to overheating when the line voltages are too low and thus the motor's current drain becomes excessive. In addition, we highly recommend having a stock of spare parts and supplies on hand for routine and emergency maintenance. These supplies include the following items:


- Powerex grease (special formulation; do not use third-party products)
- V-belts
- Replacement motor starter
- Check valves
- Safety exhaust valve
- Replacement Balston-Whatman filters

The Balston air drier originally installed on our compressed air system is still going strong, although it required a valve overhaul at the factory after about four years of continuous service. More recently, Balston-Whatman has introduced membrane air driers which reduce the dew point to only -40°C rather than -100°C but seem much more robust and less complicated than the desiccant driers. If one will be using compressed air only above -40°C , then we would suggest considering a membrane air drier since these are simpler and require less compressor capacity than the desiccant air driers.

We thank all readers who have expressed interest in our compressed air system and will be pleased to provide any details on manufacturers, installation and operation procedures, or specifications associated with this system.

Sincerely,


Ken Fishbein
Facility Manager, NMR Unit
NIH/NIA/GRC

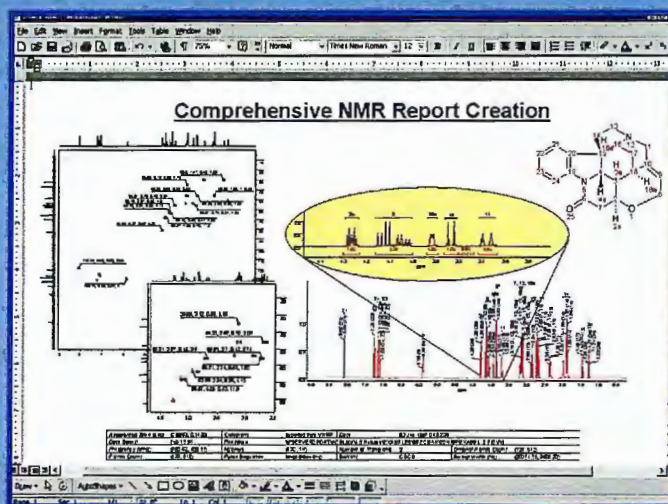

Richard G.S. Spencer
Chief, NMR Unit
NIH/NIA/GRC

Phone: (410) 558-8512
FAX: (410) 558-8376 or 8323
Email: fishbein@vax.grc.nia.nih.gov



Do you ever need to create reports like this?

ACD/SpecManager makes it possible to create reports the way YOU want them. The integrated report editor allows you to copy and paste elements of your NMR experiments directly to MS Office applications. All report objects are OLE linked, so in case you change your mind, editing is a snap! Import, process, and report your data using SpecManager's advanced capabilities.



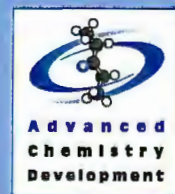
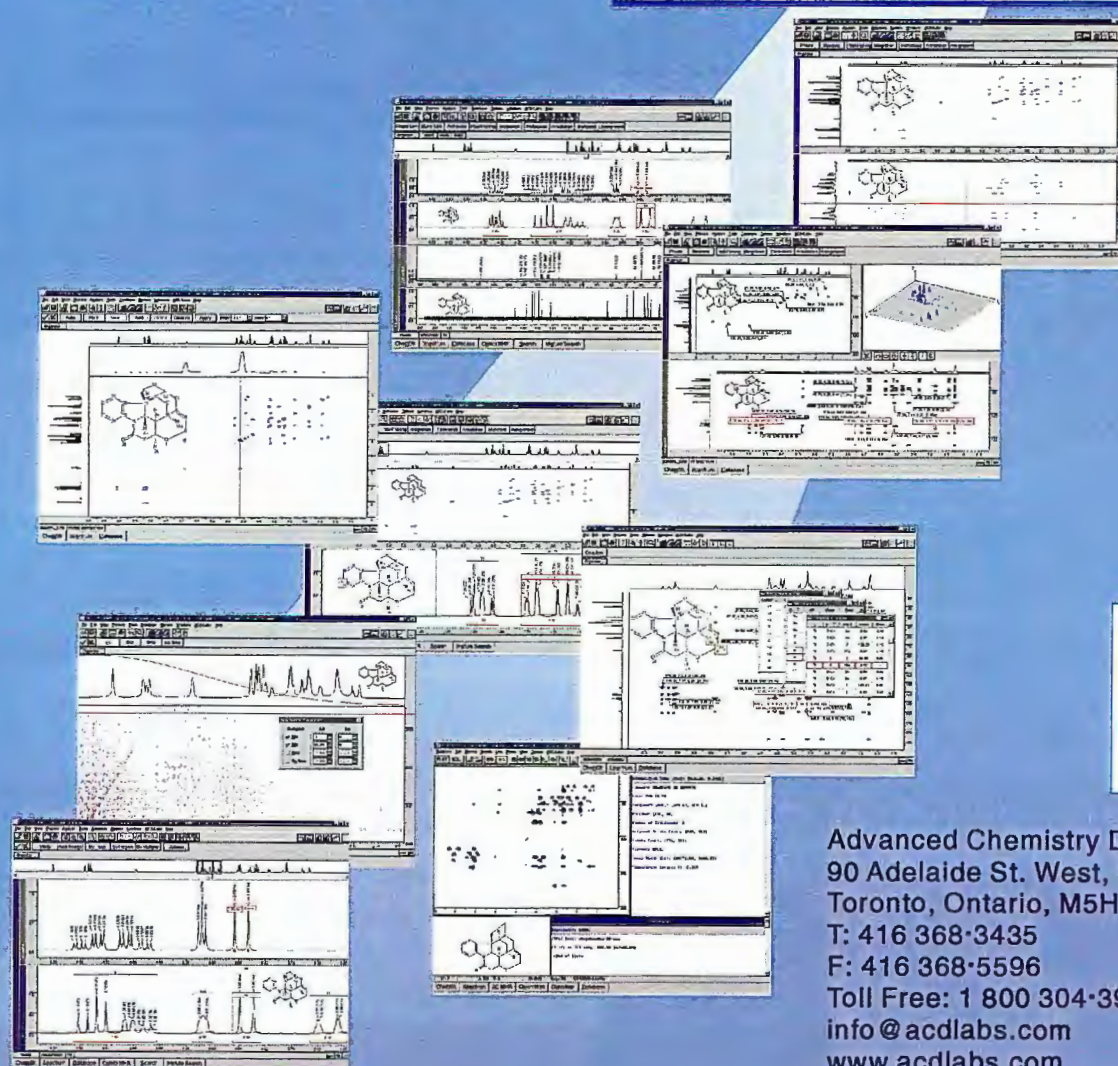
NMR

IR

UV-Vis

MS

Raman



Advanced Chemistry Development
90 Adelaide St. West, Suite 702
Toronto, Ontario, M5H 3V9, Canada
T: 416 368-3435
F: 416 368-5596
Toll Free: 1 800 304-3988
info@acdlabs.com
www.acdlabs.com



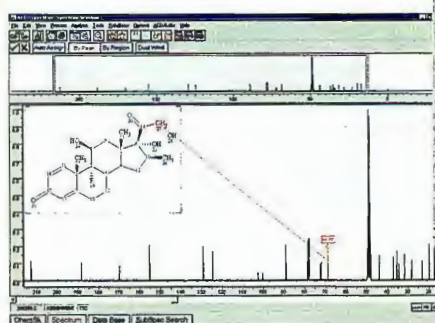
Process raw NMR data using a wide array of tools. The creation of professional reports is just a button click away!

ACD/ NMR Processor:

The NMR Processing Module of ACD/SpecManager

Don't Let Desktop
Processing Drive
You Nuts When It
Can Be So Easy!

Peak to nucleus assignment

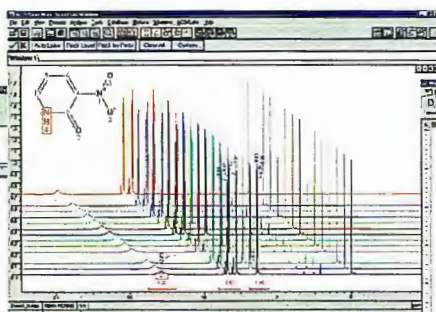


Both NMR Processor and NMR Manager provide a complete solution for processing experimental NMR data including:

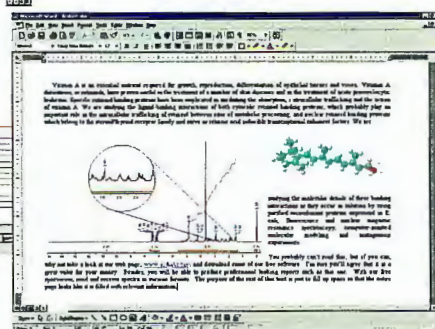
- Import the major FID and FT formats.
- Automated or manual peak picking, referencing and integration.
- View several spectra at once in Tile or Overlay Mode.

- Fourier Transform, phase correction, baseline correction, peak referencing, peak integration, and peak picking.
- Manual and auto-phasing.
- Manual and auto-integration.
- Rectangular zoom.
- Peak-by-peak assignment between structure and spectrum.
- Annotation of each spectrum using either peak or region selection is possible, offering unique capabilities to assign and annotate polymer spectra and other complex spectral curves.
- Full integration with the ChemSketch structure drawing package permits automatic layout and cut-and-paste of spectra, structures, annotations and tables.

Overlay multiple spectra



Create professional
slides and reports



ACD/2D NMR Processor

The 2D NMR Processing Module of ACD/SpecManager

A simple interface
with powerful
capabilities for 2D
processing at the
desktop!

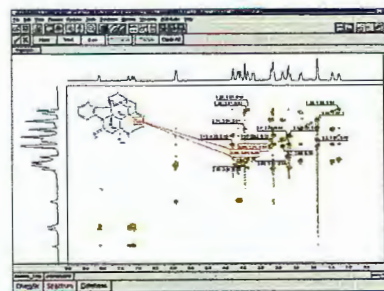
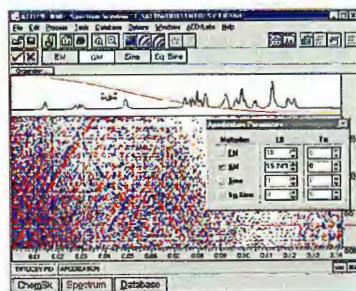
- Import different spectrometer formats (Varian, Bruker and JEOL Generic 2.0 and JCAMP-DX) and carry out Fourier Transform, zero-filling, weighting functions, phase and baseline correction,

calibration, peak picking and integration.

- **NEW**- Baseline Correction mode.
- **NEW**- Edit Spectrum mode allows editing of the entire spectrum or defined areas.
- **NEW**- Annotation mode for peaks and spectral regions.
- **NEW**- Synchronize axes of multiple windows.

- Show Magnitude spectrum or Power spectrum and perform Symmetrization.
- Apply Transpose and Reverse spectrum commands.
- View slices and 3D projections.
- Attach experimental 1D spectra to the 2D spectrum.
- Attach the chemical structure and additional data to the spectrum.
- Manually assign diagonal and cross-peaks to any atom or portion of the chemical structure.

Interactive apodization mode



Assign 2D spectra to structures

Structural Chemistry Group
Department of Chemistry

Queen Mary & Westfield College
Mile End Road, London E1 4NS

Dr. G.E. Hawkes BSc PhD CChem FRSC
Reader in Physical Organic Chemistry
Tel. 0207 882 3261, Fax 0207 882 7794
E-mail: g.e.hawkes@qmw.ac.uk
Web: <http://www.chem.qmw.ac.uk/>



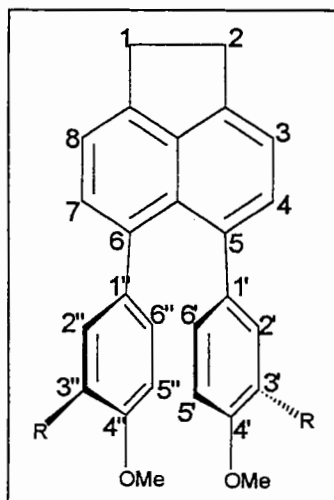
20th June 2000
(received 7/14/2000)

Prof. B.L. Shapiro,
The NMR Newsletter,
966 Elsinore Court,
Palo Alto,
CA 94303-3410, USA.

Dear Barry,

Dynamics of hindered 5,6-diarylnaphthenes

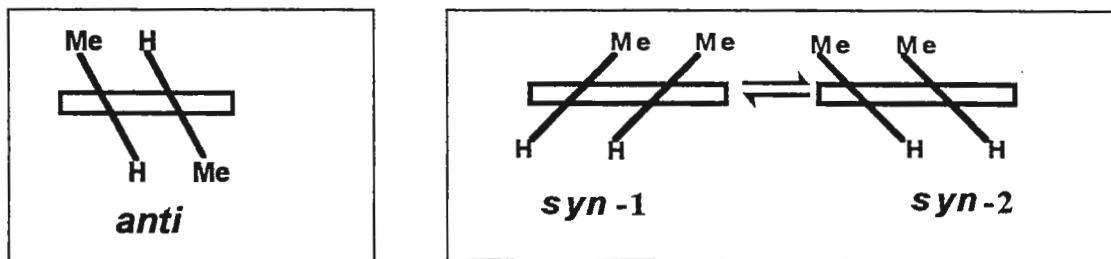
Some colleagues (Andy Whiting at UMIST, and Mike Watkinson and Romano Kroemer here at QMW) and I have been using a combination of single crystal X-ray work,



molecular modelling and ¹H NMR to study the barriers to rotation in some substituted diarylnaphthenes. When the R groups are both methyl, the compound crystallises as a single *syn* atropisomer (see below). If the R groups are both *t*-butyl the compound crystallises as the *anti* atropisomer. The modelling (quantum chemical calculations using Hartree-Fock theory and density functional theory) is in agreement with the crystallography in showing the planes of the *peri* phenyl rings to be nearly parallel, but with a dihedral angle about 60° between a phenyl ring plane

and the plane of the naphthalene part. In solution we must consider two degenerate *syn* conformers (see below) in rapid equilibrium. At low temperature (213 to 253 K in CDCl₃) separate signals due to the *syn* and *anti* atropisomers are seen and these broaden and coalesce in the range 273 to 323 K. From the low temperature NMR data for the dimethyl compound we calculate ΔH° and ΔS° for the *anti* \leftrightarrow *syn*-i, i = 1 OR 2 equilibrium; $\Delta H^\circ = -0.19 \text{ kcal mol}^{-1}$

and $\Delta S^\circ = -1.8 \text{ cal K}^{-1} \text{ mol}^{-1}$. From the exchange broadened spectra, using band-shape analysis



the rate coefficient for the exchange varied from 2.4 s^{-1} at 273 K to 452 s^{-1} at 323 K, and an Eyring plot yielded a value for the activation enthalpy, $\Delta H^* = 17.3 \text{ kcal mol}^{-1}$ and activation entropy, $\Delta S^* = 7.1 \text{ cal K}^{-1} \text{ mol}^{-1}$. The calculated activation energy for the interconversion was $17.9 \text{ kcal mol}^{-1}$ (HF/3-21G) or $13.2 \text{ kcal mol}^{-1}$ using DFT (B3LYP). The Hartree-Fock calculation gave the better correlation with experiment. The experimental and calculated (HF) activation parameters for the di-*t*-butyl compound were very similar (within 1 kcal mol^{-1}), indicating that the process does not involve a clash of the substituent alkyl groups. A third compound was prepared with R = *t*-butyl and with additional methyl groups at the 5' and 5'' positions, in an attempt to raise the barrier significantly. However the barrier was only slightly increased - experimental $\Delta H^* = 20.5 \text{ kcal mol}^{-1}$ and $\Delta S^* = 13.9 \text{ cal K}^{-1} \text{ mol}^{-1}$, and HF-calculated $18.9 \text{ kcal mol}^{-1}$. Modelling of the transition state showed significant non-planarity of the naphthalene ring system, and this distortion increases the distance between the phenyl rings thereby reducing steric repulsion in the transition state. One significant conclusion is that bulky substituents in the meta positions (3'/3'' and 5'/5'') are not capable of stabilising a single atropisomeric form.

Best wishes.

Yours sincerely,

Dr. G.E. Hawkes

Rima Nasser

STABLE ISOTOPE DERIVATIVES OF PHOSPHOLIPIDS

Available from Avanti

PHOSPHOLIPID DERIVATIVES

Phosphatidylcholine
Phosphatidylethanolamine
Phosphatidylglycerol
Phosphatidic Acid
Phosphatidylserine

Dodecyl Phosphocholine

Lyso Phosphatidylcholine

Mixed fatty acid derivatives
*Unlabeled saturated, unlabeled monoene
or unlabeled polyene fatty acids in the
one or two position of glycerol*

POSITION OF STABLE ISOTOPE

Carbon 13
Carbonyl Carbon

Deuterium

Perdeuterated Fatty Acids
6:0 - 12:0 - 14:0 - 16:0 - 18:0

Perdeuterated Alkyl Chains
6:0 - 12:0 - 14:0

Choline
Ethylene Bridge
Methyl Groups
Perdeuterated

See over for structures of typical products

VISIT OUR WEB SITE AND DOWNLOAD A COPY OF OUR LATEST CATALOG
FEATURING OVER 1,000 LIPID BASED RESEARCH PRODUCTS.



Avanti®
POLAR LIPIDS, INC.

700 INDUSTRIAL PARK DRIVE, ALABASTER, AL 35007

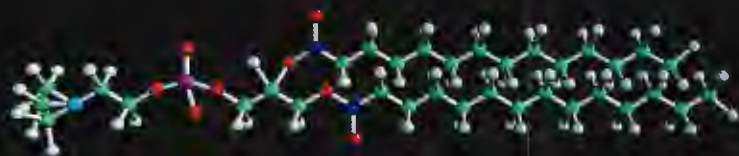
FAX 205-663-0756 • E-MAIL INFO@AVANTILIPIDS.COM • WEB SITE WWW.AVANTILIPIDS.COM

**For information about Avanti please contact our
Product Hotline: 800-227-0651 (USA & Canada) or 205-663-2494 International**

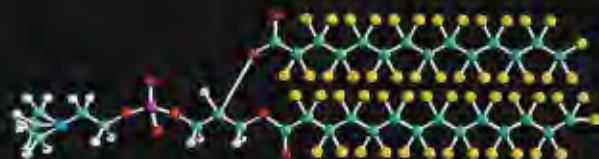
Stable Isotope Derivatives

SYMMETRIC FATTY ACID

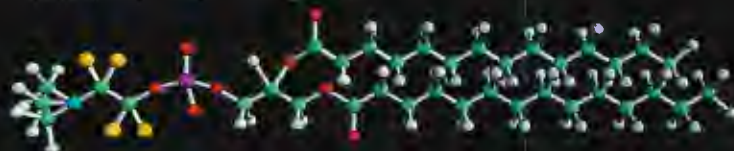
- ALSO AVAILABLE IN PALMITOYL & STEAROYL



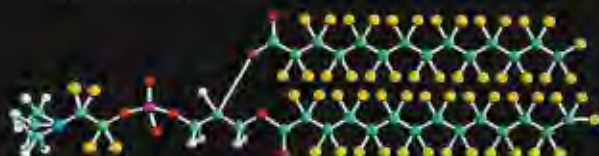
CARBON 13 14:0 PC



14:0 PC (D54)



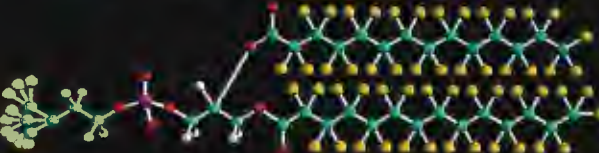
14:0 PC (D4)



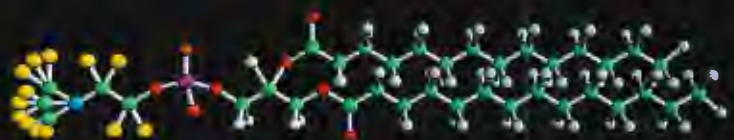
14:0 PC (D58)



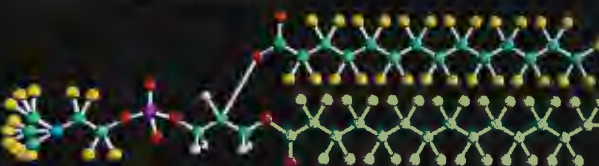
14:0 PC (D9)



14:0 PC (D63)

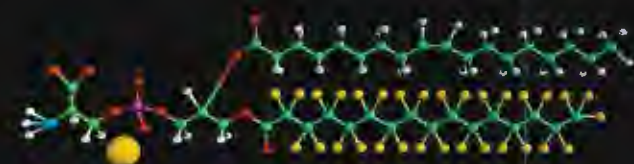


14:0 PC (D13)

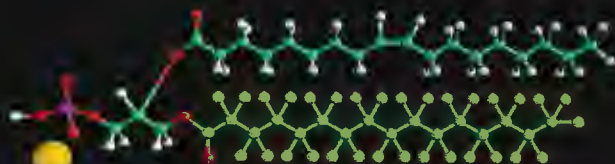


14:0 PC (D67)

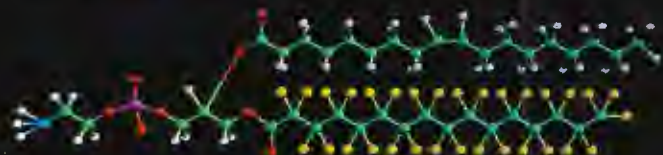
ASYMMETRIC FATTY ACID



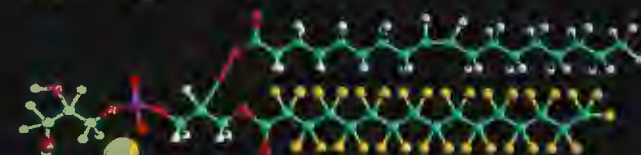
16:0-18:1 PS (D31)



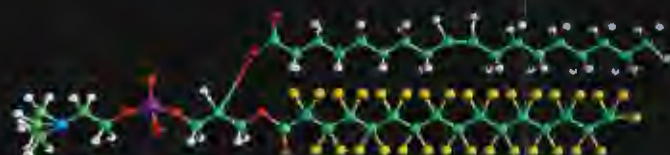
16:0-18:1 PA (D31)



16:0-18:1 PE (D31)



16:0-18:1 PG (D31)



16:0-18:1 PC (D31)



Avanti[®]
POLAR LIPIDS, INC.

PHARMACIA



Gary E. Martin, Ph.D.
Distinguished Scientist & Group Leader
Rapid Structure Characterization Group
Pharmaceutical Development
MS#4821-259-277
(616) 833-6283 (voice)
(616) 833-6743 (fax)
gary.e.martin@am.pnu.com : e-mail

(received 7/14/2000)
June 29, 2000

Bernard L. Shapiro, Ph.D.
Editor, The NMR Newsletter
966 Elsinore Court
Palo Alto, CA 94303

**$^2J, ^3J$ -HMBC: Unequivocal
Differentiation of $^2J_{CH}$ from $^3J_{CH}$ Long-range
Correlations to Protonated Carbons**

Dear Barry,

Continuing with the development of new, accordion-optimized, long-range heteronuclear shift correlation experiments, we'd like to take this opportunity to describe the $^2J, ^3J$ -HMBC experiment.¹ This new, proton-detected, long-range experiment provides the means of unequivocally differentiating two-bond from three-bond correlations to protonated carbons. Our new experiment has its origin quite a number of years ago, in 1985 to be specific, when a number of labs were engaged in the development of new long-range heteronuclear shift correlation experiments.² In one report, Reynolds described an experiment that he called XCORFE.³ That experiment utilized a BIRD pulse to provide the means of differentiating, in a heteronucleus-detected long-range experiment (Ad wouldn't give us the gift of HMBC for another year!), two-bond from three-bond long-range correlations to protonated carbons. The experiment which we now report, $^2J, ^3J$ -HMBC, incorporates a BIRD pulse within a constant time variable delay first introduced in the IMPEACH-MBC experiment⁴ and subsequently modified with the recently reported CIGAR-HMBC experiment⁵ to accomplish the same task. The BIRD pulse is used much as in the XCORFE experiment³ to selectively manipulate particular components of magnetization, thereby providing the basis for differentiation between two-bond and three-bond long-range heteronuclear correlations. The new operator has been given the acronym STAR (Selectively Tailored Accordion F_1 Refocusing), and is incorporated within the constant time variable delay. The experiment also incorporates the idea of Jscaling to enhance the differentiation of two- and three-bond long-range correlations as introduced with the CIGAR-HMBC experiment.⁵

The constant time variable delay, as employed in the IMPEACH-MBC⁴ experiment and further refined in the CIGAR-HMBC⁵ experiment is shown in Figure 1. The constant time variable delay is contained within the shaded area of the pulse sequence. Despite its' rather oxymoronic name, this pulse sequence element has a constant time for the evolution of homonuclear coupling modulations, which eliminates this modulation. At the same time the pulse sequence element serves as a variable delay for the heteronuclear couplings of interest which are to be sampled in an accordion fashion in the experiment. The idea of accordion-optimized long-range delays was introduced in the work of Wagner and Berger in their description of the ACCORD-HMBC experiment.⁶ Our more rigorous analysis of ACCORD-HMBC⁷ led to the determination that F_1 response "skew" is a function of the optimization range of the experiment, the number of increments of the evolution time used to digitize the second time domain, and the spectral width in the second dimension. The unfortuitous choice of parameters for an ACCORD-HMBC experiment,⁷ can lead to long-range response overlap in the second frequency domain as a result of responses that can be several kilohertz in width in F_1 . Conversely, the F_1 skew of long-range responses can be used as a determinant of response authenticity, as noise and other random events are not subject to proton homonuclear coupling modulation during the variable delay of the ACCORD-HMBC experiment, and are thus not subject to F_1 skew.

The first portion of the constant time variable delay is an interval, D, is split by a $180^\circ ^{13}C$ pulse. The second portion of the pulse sequence element is a variable delay, vd, analogous to that in the ACCORD-HMBC experiment. F_1 modulation in ACCORD-HMBC experiments arises as a function of homonuclear 1H frequency modulation during the variable delay, vd,

which serves as a pseudo-evolution period for this process.^{4,7} By keeping the overall delay duration constant, ^1H frequency modulation, obviously, can be suppressed.^{4,5} To allow the sampling of a range of potential heteronuclear long-range couplings, however, the duration of time interval during which heteronuclear couplings are sampled must be of variable duration. To achieve these seemingly conflicting objectives, the constant time variable delay first maintains the overall time constant to suppress ^1H frequency modulation. As the duration of vd is decremented with successive increments of the evolution time, t_1 , the overall duration of the delay, D , is incremented by the same amount. To sample heteronuclear couplings using a variable duration delay, the 180° ^{13}C pulse at $D/2$ refocuses the heteronuclear couplings at D . Hence, heteronuclear couplings evolve only during the variable portion of the delay represented by vd . In this fashion, as the duration of vd is successively decremented in successive increments of the evolution time, t_1 , thus, the sampling of a range of long-range couplings is facilitated in a manner analogous to the ACCORD-HMBC experiment.^{6,7}

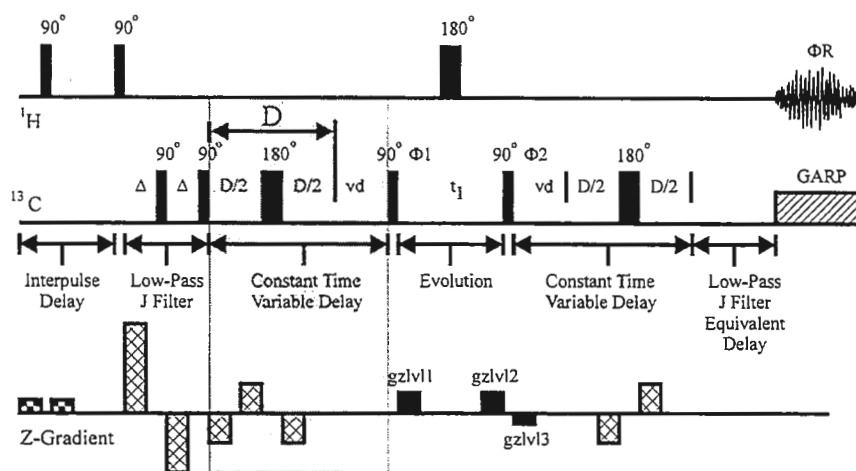


Figure 1. IMPEACH-MBC pulse sequence.⁴ The constant duration of the constant time variable delay (high-lighted region prior to evolution and identical unhighlighted component following evolution) suppresses F_1 modulation characteristic of the ACCORD-HMBC experiment. Heteronuclear long-range couplings are allowed to evolve only during the variable, vd , portion of the constant time variable delay. In this fashion, a range of long-range couplings can be sampled in the experiment despite the constant duration of the time interval. The phase of the unlabeled pulses in the sequence was held constant at 0.

The cycled phases were: $\Phi_1 = 0202$; $\Phi_2 = 0202$; $\Phi_R = 0220$. Gradient ratios were $2 : 2 : 27 : -18 : -9 : 9 : -9 : 2 : 2 : -1$ G cm^{-1} . The sequence shown allows broadband X-decoupling during acquisition. If decoupling is not desirable, the second set of constant time variable delays and the low-pass J-filter equivalent delay can be eliminated, thereby improving sensitivity.

The IMPEACH-MBC experiment successfully eliminated the problem of potential long-range response overlap inherent to the ACCORD-HMBC experiment. With IMPEACH-MBC, it was possible to digitize as dictated by resolution requirements of the sample being studied in the second frequency domain rather than having to resort to high digitization in the second time/frequency domain as a means of partially ameliorating the problems of response modulation. The downside of the IMPEACH-MBC experiment, unfortunately, was to rob the investigator of the first real means of response authentication for weak responses.⁴ The subsequently reported CIGAR-HMBC experiment was fashioned to allow the reintroduction of a user-determined amount of F_1 response modulation for use as a determinant of response authenticity.⁵

The CIGAR-HMBC pulse sequence is shown below in Figure 2. The fundamental difference between CIGAR-HMBC and the predecessor IMPEACH-MBC experiment is in the manipulation of the delays during the constant time variable delay. As will be noted by examining the shaded segment of the figure, the delays flanking the 180° ^{13}C pulse during the constant time variable delay are no longer the simple $D/2$ delay used in the IMPEACH-MBC experiment.⁴ The $D/2$ segments of the delay are still present but are now incremented by $(\tau_{\text{max}} - \tau_{\text{min}})/n_i$ (where n_i = the number of increments of the evolution time, t_1) as in the IMPEACH-MBC experiment in concert with the decrementation of the variable portion of the delay, vd . The delays flanking the 180° ^{13}C pulse are further manipulated to reintroduce user-defined F_1 modulation by incrementing the delay by a further $\Delta 2/2$, where $\Delta 2$ is defined as $(J_{\text{scale}} - 1)t_1$. This additional incrementation reintroduces a pseudo-evolution time of user-determined duration for proton homonuclear coupling modulation analogous to that which is present in a parameter dependent manner in the ACCORD-HMBC experiment.⁷

Voltronics non-magnetic trimmer capacitors:



More than
34 years of
fine tuning

The first choice for NMR and MRI probes

Every NMR and MRI Test Depends on One Moveable Part!

Features

- They're truly non-magnetic, with magnetic field distortion less than 1 part per 600 million.
- Lifetime is far greater and RF power handling capability higher thanks to our non-rotating piston design.
- Tuning is linear - no reversals.
- Positive stops at minimum and maximum capacitance.
- Extended shafts can be specified because the tuning screw does not move in or out.

Specifications

| | |
|---------------------------|-----------------------------|
| Frequency range | to 1.5 GHz |
| Working Voltage | to 20 kV |
| Capacitance ranges | 0.45 pF min. to 120 pF max. |
| Sizes | From 0.12 in. to 1 in. dia. |
| Mounting styles | All common types |
| Magnetic field distortion | <1 part per 600 million |

Custom is Standard at Voltronics

Every NMR and MRI system has unique requirements, and we address them all. In fact we built our entire line of non-magnetic trimmers based on specific requests from our customers. We'll gladly modify an existing trimmer design or create a new one to meet the exact needs of your system.

So if you're building NMR or MRI systems, you should be talking to Voltronics. For 25 years, we've delivered the best-performing, most reliable non-magnetic trimmer capacitors available.

Call (973) 586-8585 and discuss your needs with one of our applications engineers.

Voltronics 
CORPORATION
The Trimmer Capacitor Company

100-10 Ford Road • Denville, NJ 07834
973.586.8585 • FAX: 973.586.3404
e-mail: info@voltronicscorp.com
Our complete catalog can be found at:
<http://www.voltronicscorp.com>

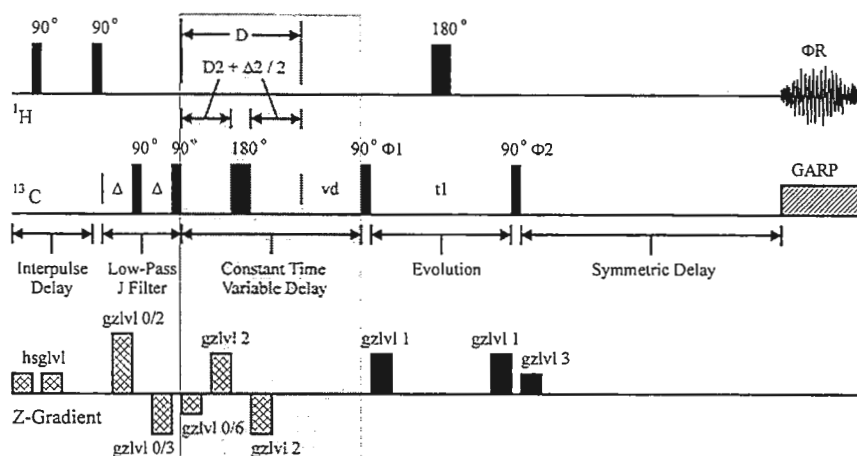


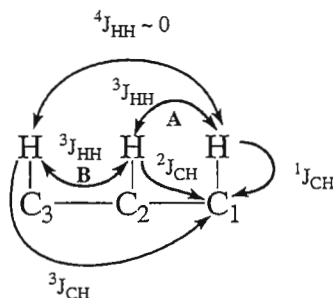
Figure 2. CIGAR-HMBC pulse sequence.⁵ The modified constant duration of the constant time variable delay (highlighted region prior to evolution) allows the introduction of user-defined F_1 modulation characteristics like those inherent to long-range responses in the ACCORD-HMBC experiment. Heteronuclear long-range couplings are allowed to evolve only during the variable, vd , portion of the constant time variable delay as in the IMPEACH-MBC experiment.⁴ The delay, D , which is halved to flank the 180° ^{13}C pulse at $D/2$ in the constant time variable delay is

first manipulated by incrementation as in the IMPEACH-MBC experiment (*i.e.* by $(\tau_{\max} - \tau_{\min})/n_i$ where n_i = the number of increments of the evolution time, t_1). The duration of D is further manipulated by the addition of the term $\Delta 2$, where $\Delta 2$ is defined as $(J_{\text{scale}} - 1)t_1$. The term J_{scale} is the user-selected scaling parameter and t_1 is the evolution time as usual. The phase of the unlabeled pulses in the sequence was held constant at 0. Phases of the other pulses are as follows: $\Phi_1 = 0202$; $\Phi_2 = 0022$; $\Phi_R = 0220$. Again, if broadband X-decoupling during acquisition is not desired, the symmetric delay interval can be eliminated to improve sensitivity.

There are three possible choices for the parameter J_{scale} in a CIGAR-HMBC experiment. First, by setting $J_{\text{scale}} = 0$, the overall duration of $D/2 + \Delta 2/2$ is decremented by the $\Delta 2/2$ term. Choosing this value of J_{scale} provides an experiment with a constant overall duration, which completely eliminates the small homonuclear coupling modulation inherent to both HMBC/GHMBC and IMPEACH-MBC. In this sense, when $J_{\text{scale}} = 0$, the CIGAR-HMBC experiment performs in a fashion analogous to the CT-HMBC experiments described by Furihata and Seto.⁸ This choice affords the highest possible F_1 resolution. Next, setting $J_{\text{scale}} = 1$ gives an experimental result that is identical to that obtained with the IMPEACH-MBC experiment. The F_1 modulation inherent to the ACCORD-HMBC experiment is suppressed, the homonuclear modulation which arises from the incrementation of the evolution period, t_1 , is unaffected. Finally, and most interesting, are the results which are obtained when the CIGAR-HMBC experiment is performed with $J_{\text{scale}} > 1$. In this case, as described above, user-determined F_1 skew is reintroduced as a characteristic of the long-range correlation responses that can serve as a determinant of response authenticity. Spectral segments extracted from five spectra (ACCORD-HMBC, CIGAR-HMBC with $J_{\text{scale}} = 0, 5$, and 10, and IMPEACH-MBC) are shown, and discussed comparatively in Figure 3.

The ability to control F_1 skew by the user-selected parameter J_{scale} increases the utility of the CIGAR-HMBC experiment considerably relative to the IMPEACH-MBC experiment. In particular, the ability to introduce a controlled amount of F_1 skew into the spectrum returns to the investigator a powerful means of long-range response authentication. Response authentication can be extremely useful in the case of weak, long-range responses, *e.g.* $^4J_{\text{CH}}$ correlations which are frequently observed in accordion-optimized long-range experiments when broad excitation ranges are employed. Further, relative to the ACCORD-HMBC experiment, the CIGAR-HMBC also has the advantage of F_1 response skew being independent of the number of increments selected to digitize the second frequency domain.

The experimental developments in accordion-optimized long-range experiments over the past year set the stage for the current modification of the constant time variable delay contained in the $^2J, ^3J$ -HMBC experiment. The constant time variable delay is further modified by the incorporation of the STAR operator (Selectively Tailored Accordion F_1 Rescaling) shown in Figure 3.



1

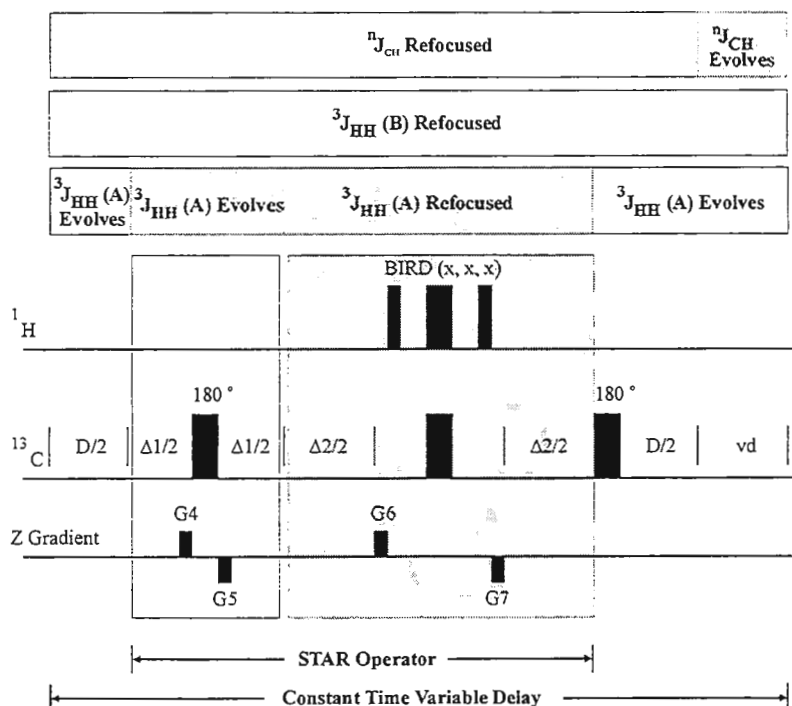


Figure 3. STAR Operator (Selectively Tailored Accordion F_1 Refocusing) shown within a constant time variable delay. Heteronuclear long-range components of magnetization are refocused at the end of the D, $\Delta 1$, and $\Delta 2$ segments of the pulse sequence operator by the 180° ^{13}C pulses located midway through each of the segments. Long-range heteronuclear couplings are sampled only during the variable portion (for them) of the delay, vd. Vicinal proton-proton homonuclear couplings of the type $^3J_{\text{HH}}(\text{B})$ shown for **1** evolve in constant time over both the STAR operator and throughout the constant time variable delay. Thus, these responses have no F_1 skew. In contrast, vicinal proton-proton homonuclear couplings of the type $^3J_{\text{HH}}(\text{A})$ are manipulated rather differently during the STAR operator. The BIRD pulse centered in $\Delta 2$ is selective for protons directly bound to ^{13}C . Hence, these protons are refocused during the $\Delta 2$ interval of the experiment.

The duration of the $\Delta 1$ interval of the STAR operator begins at zero and is incremented to $J_{\text{scale}} \times t_{1\text{max}}$ (where $t_{1\text{max}}$ is the acquisition time in F_1) by steps of $J_{\text{scale}} \times t_1$. The duration of $\Delta 2$, in contrast, begins at $J_{\text{scale}} \times t_{1\text{max}}$ and is decremented to zero in steps of $J_{\text{scale}} \times t_1$, keeping the overall duration of the STAR operator constant. Since the vicinal couplings $^3J_{\text{HH}}(\text{A})$ are refocused by the BIRD pulse centered in $\Delta 2$, these homonuclear couplings evolve in variable time during the $\Delta 1$ interval of the STAR operator (shaded areas of bar above the pulse sequence operator). As in the ACCORD-HMBC experiment,⁷ the evolution of homonuclear couplings in variable time leads to F_1 skew for the associated long-range heteronuclear coupling. In this case, however, the F_1 skew is associated exclusively with two-bond long-range heteronuclear couplings, *e.g.* the two-bond coupling of $\text{C}_2\text{H}-^{13}\text{C}_1$ as shown by **1**. Four bond homonuclear couplings, where $^4J_{\text{HH}} \sim 0$ Hz, are not expected to be affected by the operation of the STAR operator.

The incorporation of the constant time variable delay containing the STAR operator is shown in Figure 4. The dual stage gradient low pass J-filters employs gradients G1-G3, which must sum to zero (*e.g.* 15, -10, -5 Gcm^{-1}). The gradients during the $\Delta 1$ and $\Delta 2$ intervals, G4/G5 and G6/G7, are applied and set pairwise and must also sum to zero (*e.g.* 10, -10 Gcm^{-1}). Gradients G8-G10 are the coherence selection gradients and are applied, as usual, in a 2:2:1 ratio for $^1\text{H}-^{13}\text{C}$ or 5:5:1 for $^1\text{H}-^{15}\text{N}$ correlation experiments (or comparable ratios). The phase of the 90° ^{13}C pulse that precedes evolution and the receiver are cycled as 0202; the phase of all other pulses are held at 0.

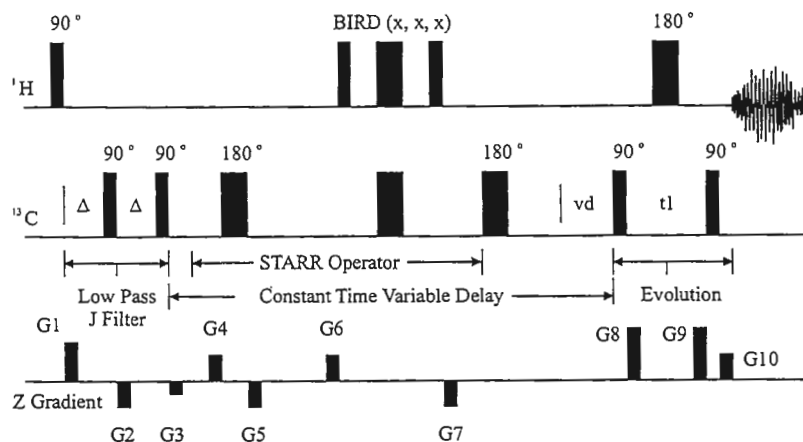
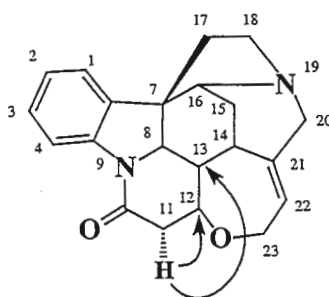


Figure 4. Complete $^2J, ^3J$ -HMBC pulse sequence schematic. Gradients during the gradient dual-stage low-pass J-filter are set to sum to zero (e.g. 15, -10, -5 Gcm $^{-1}$); the pairwise gradients flanking the 180° ^{13}C pulse applied during $\Delta 1$ and flanking the BIRD pulse centered in $\Delta 2$ also must sum to zero. The coherence selection gradients, G8-G10, are applied in a 2:2:1 ratio (or a comparable ratio) for ^1H - ^{13}C or 5:5:1 for ^1H - ^{15}N . The duration of the $\Delta 1$ and $\Delta 2$ intervals (see Figure 3) is established as a function of J_{scale} and $t_{1\text{max}}$. The phase of the 90° ^{13}C pulse that precedes the evolution period, t_1 , and the receiver phase are cycled as 0202; the phase of all other pulses is held constant.

To illustrate schematically, the results expected from the $^2J, ^3J$ -HMBC experiment, consider long-range correlations of the H-11 α resonance of strychnine (**2**) to C-12 and C-13 *via* two- and three-bonds, respectively. Because of the operation of the STAR operator, the homonuclear coupling between H-11 α -H12 is decoupled during $\Delta 2$, leading to evolution in variable time during the $\Delta 1$ interval of the STAR operator. This leads to the selective F_1 skew of the $^2J_{\text{CH}}$ long-range response correlating H-11 α -C12. The vicinal coupling between H-12-H-13 is unaffected by the STAR operator, allowing this coupling to evolve in constant time. Hence, the H-11 α -C-13 $^3J_{\text{CH}}$ correlation response is unaffected by the STAR operator and does not exhibit F_1 skew. These responses are illustrated schematically in Figure 5. A plot of the aliphatic region of the $^2J, ^3J$ -HMBC spectrum of strychnine is shown in Figure 6.



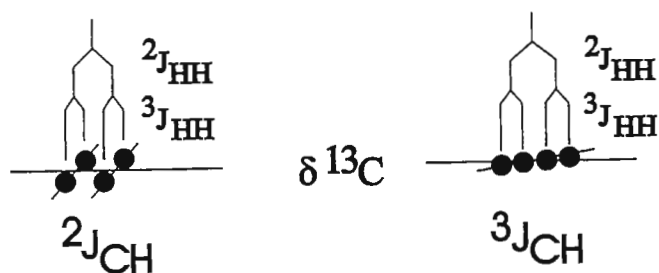


Figure 5. Schematic representation of the expected response appearance for the ${}^2J_{CH}$ coupling of H-11 α to C-12 vs. the ${}^3J_{CH}$ correlation to C-13. Homonuclear coupling between H-11 α -H12 is decoupled during $\Delta 2$ in the STAR operator leading to evolution in variable time during the $\Delta 1$ interval of the STAR operator for this homonuclear vicinal coupling. This leads to the selective F_1 skew of the ${}^2J_{CH}$ long-range response correlating H-11 α -C12. The vicinal coupling between H-12-H-13 is unaffected by the STAR operator, hence, the H-11 α -C-13 ${}^3J_{CH}$ correlation response is unaffected and does not exhibit F_1 skew.

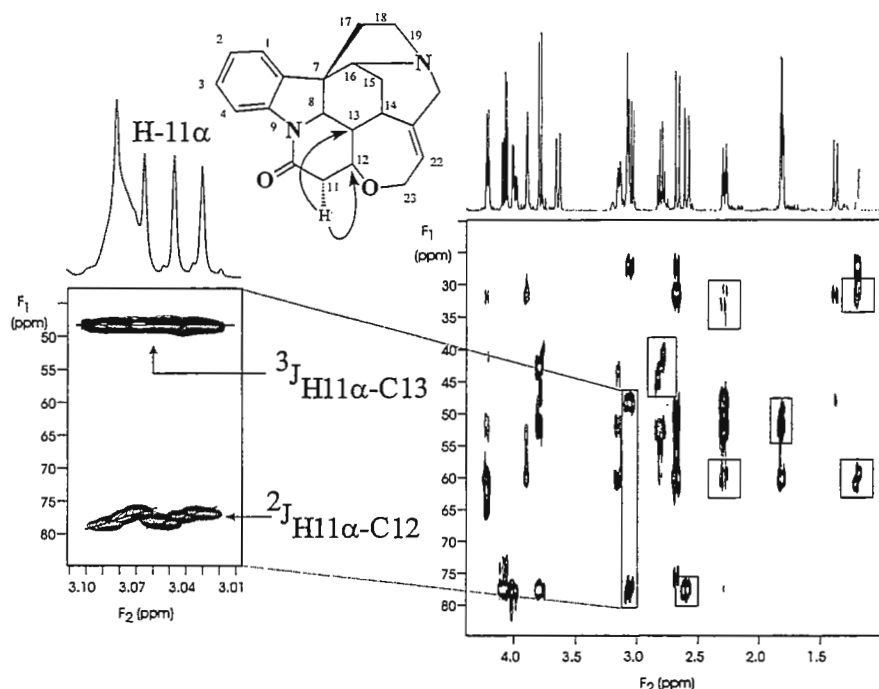




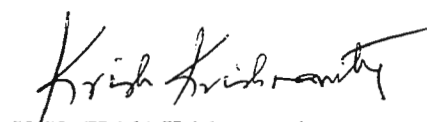
Figure 6. ${}^2J, {}^3J$ -HMBC spectrum of the aliphatic region of strychnine (2). The experiment was run with the parameter $J_{scale} = 16$; the accordion optimization range of the variable delay was from 6 (83 msec) to 10 (50 msec) Hz. Data were acquired as 2048 x 128 points with spectral widths in F_2 and F_1 of 4,454 and 28269 Hz, respectively. Two-bond correlation responses exhibiting characteristic F_1 skew (see Figure 4) are enclosed in boxes in the right panel. The long-range correlations from H-11 α to C-12 and C-13 are shown in the expansion in the left panel to show detail.

The degree of F_1 skew exhibited by ${}^2J_{CH}$ responses is "adjusted" by the parameter J_{scale} as shown in Figure 7. As larger values of J_{scale} are employed, a progressively greater degree of F_1 skew is exhibited by two-bond correlation responses. The value of J_{scale} should, however, be used judiciously since there are signal losses associated with lengthening the duration of the components of the STAR operator when large values of J_{scale} are utilized.


Gary E. Martin


David J. Russell


Chad E. Hadden


V. V. (Krish) Krishnamurthy
Varian, Inc.

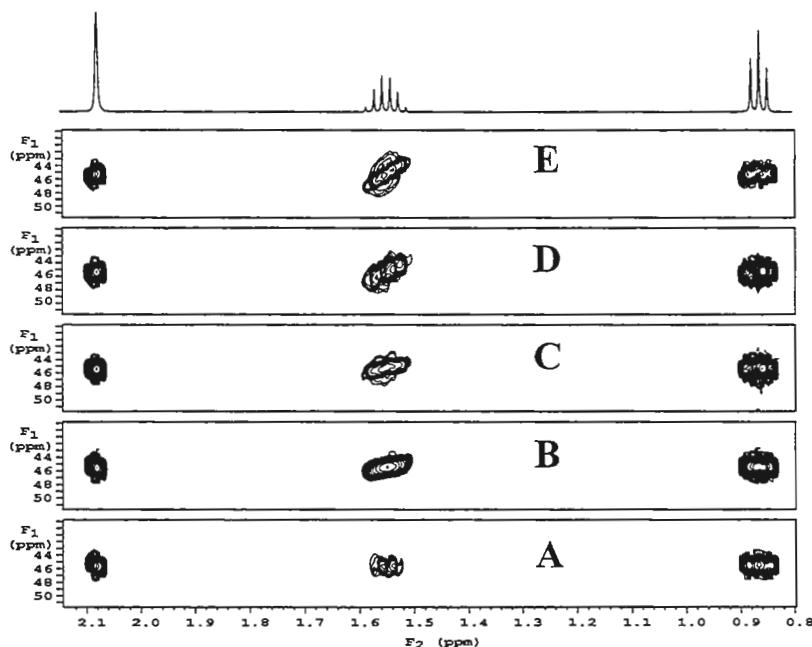


Figure 7. ${}^2J, {}^3J$ -HMBC segments showing correlations to the C-3 resonance of 2-pentanone. The ${}^2J_{CH}$ correlation from H4-C3 shows (1.55 ppm) shows the effect of increasing the value of the parameter J_{scale} . All panels were taken from experiments performed taking 2048 x 128 points with an accordion optimization range of 6-10 Hz.

Panel A) $J_{scale} = 0$

Panel B) $J_{scale} = 6$

Panel C) $J_{scale} = 12$

Panel D) $J_{scale} = 18$

Panel E) $J_{scale} = 24$

References

- 1) V.V. Krishnamurthy, D.J. Russell, C.E. Hadden, and G.E. Martin, *J. Magn. Reson.*, in press (2000).
- 2) Heteronucleus-detected long-range chemical shift correlation methods have been reviewed: G.E. Martin and A.S. Zektzer, *Magn. Reson. Chem.*, **26**, 631-652 (1988).
- 3) W.F. Reynolds, D.W. Hughes, M. Perpich-Dumont, and R.G. Enriquez, *J. Magn. Reson.*, **63**, 413-417 (1985).
- 4) G.E. Martin, C.E. Hadden, and V.V. Krishnamurthy, *The NMR Newsletter*, No. 488, pp. 11-14 (1999); C. E. Hadden, G. E. Martin, and V. V. Krishnamurthy, *J. Magn. Reson.*, **140**, 274-280 (1999).
- 5) G.E. Martin, C.E. Hadden, D.J. Russell, and V.V. Krishnamurthy, *The NMR Newsletter*, No. 495, pp. 11-15 (1999); C.E. Hadden, G.E. Martin, and V.V. Krishnamurthy, *Magn. Reson. Chem.*, **38**, 143-147 (2000).
- 6) R. Wagner and S. Berger, *Magn. Reson. Chem.*, **36**, S44 (1998).
- 7) G. E. Martin, C. E. Hadden, R. C. Crouch, and V. V. Krishnamurthy, *The NMR Newsletter*, No. 487, pp. 11-13 (1999); G. E. Martin, C. E. Hadden, R. C. Crouch, and V. V. Krishnamurthy, *Magn. Reson. Chem.*, **37**, 517-529 (1999).
- 8) K. Furihata and H. Seto, *Tetrahedron*, **37**, 8901 (1996).

Positions Available

Pharmacia Corporation is a global pharmaceutical company with an R&D pipeline of exceptional strength and depth. Our research philosophy values creativity, scientific rigor, teamwork, and personal as well as professional satisfaction. We invite you to be an integral member of our scientific team. The following opportunities are available in the structural chemistry NMR group at Pharmacia Corporation's Kalamazoo, MI facility.

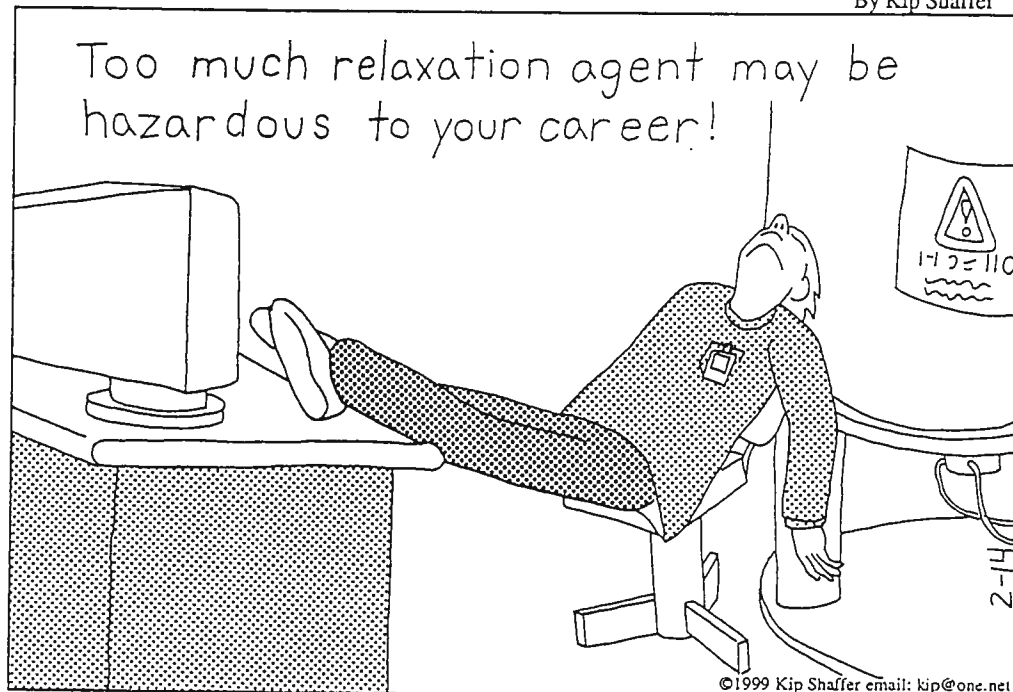
Position #901129. This position requires a Ph.D. in Biochemistry, Biophysics or Chemistry. As a member of the structural chemistry NMR group you will impact drug discovery and drug design projects by identifying lead chemical templates and determining the structures of proteins or protein/ligand complexes. The successful candidate will have considerable experience in NMR instrumentation, methods and pulse sequence development, including multidimensional heteronuclear experiments, as applied to ligand screening or protein structure determination. Experience in all aspects of protein NMR spectroscopy, including data collection, data analysis and determination of solution structures is required. Strong publications history and communication skills are required.

Position #901131. This position requires an M.S. in Biochemistry, Biophysics or Chemistry or B.S. with a minimum of 2 years of experience with NMR spectroscopy. As a member of the structural chemistry NMR group you will impact drug discovery and drug design projects by identifying and evaluating lead chemical templates. The successful candidate will develop, implement and apply NMR screening methodologies, and will interface with the biological and chemical communities to conduct detailed studies of protein/ligand interactions. Experience in flow NMR instrumentation as applied to ligand screening, as well as modern NMR methods used to study protein/ligand interactions, is highly desired. Excellent communication, data management and technical writing skills are required.

If you can meet our high expectations, you can make a real difference with Pharmacia Corporation. For confidential consideration, please indicate the position # that you are applying for and email or mail your resume to: brian.j.stockman@am.pnu.com or Dr. Brian J. Stockman, Pharmacia Corporation, Structural, Analytical & Medicinal Chemistry, 301 Henrietta St., Kalamazoo, MI 49001. An equal opportunity employer, we value a diverse combination of ideas, perspectives, and cultures.

Field of Dreams

By Kip Shaffer



Department of Biochemistry

July 24, 2000

(received 7/28/2000)

Dr. B.L. Shapiro
The NMR Newsletter
966 Elsinore Court
Palo Alto, CA 94303-3410

Position Available

Dear Barry: It has been a crazy couple of months, during my re-location to Wake Forest University School of Medicine (Bowman-Gray). It took a few weeks for my furniture to find my new home and by then my wife had a new baby boy (Karl Henry Gmeiner, our third boy, so much for NMR spectroscopists having girls). Anyways, I am now Chair of the Biochemistry Department here, and we plan on recruiting an Assistant Professor (tenure-track) in the area of NMR Spectroscopy of proteins. Interested individuals may send their CV and names of two references to:

William H. Gmeiner
Professor and Chair
Department of Biochemistry
Wake Forest University School of Medicine
Medical Center Boulevard
Winston-Salem, NC 27157-1016

Sincerely yours,

Bill

William H. Gmeiner, Ph.D.
Professor and Chair

**Address all Newsletter
correspondence to:**

Dr. B. L. Shapiro
The NMR Newsletter
966 Elsinore Court
Palo Alto, CA 94303.
650-493-5971* - Please call
only between 8:00 am and
10:00 pm, Pacific Coast time.

Deadline Dates

| | |
|-----------------|---------------|
| No. 504 (Sept.) | 24 Aug. 2000 |
| No. 505 (Oct.) | 27 Sept. 2000 |
| No. 506 (Nov.) | 27 Oct. 2000 |
| No. 507 (Dec.) | 24 Nov. 2000 |
| No. 508 (Jan.) | 22 Dec. 2000 |

* Fax: 650-493-1348, at any hour. Do not use fax for technical contributions to the Newsletter, for the received fax quality is very inadequate.

* E-mail: shapiro@nmrnewsletter.com

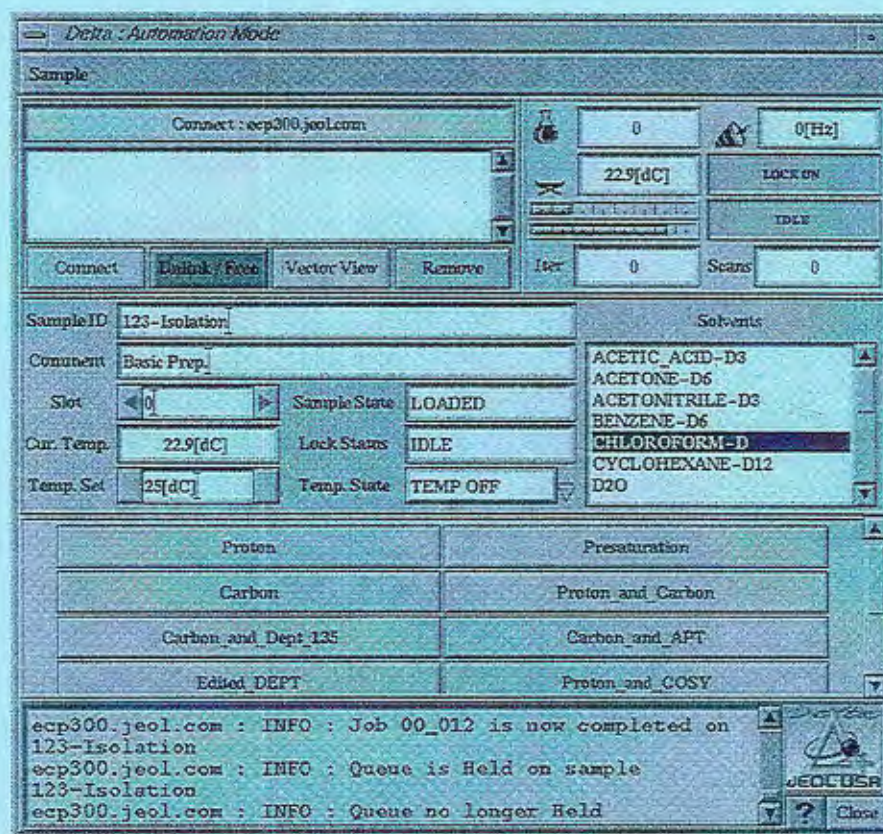


The Newsletter's fiscal viability depends very heavily on the funds provided by our Advertisers and Sponsors. Please do whatever you can to let them know that their support is noted and appreciated.

Mailing Label Adornment: Is Your Dot Red ?

If the mailing label on your envelope is adorned with a large red dot: this decoration means that you will not be mailed any more issues until a technical contribution has been received.

JEOL Can Give You the Data You Need From Your Desktop PC or MAC



The **Eclipse+** NMR Spectrometer can be operated anywhere there is a computer on the local network. The **Single Window Automation** pictured above can be used with a single mouse click to select the sample from the auto-sample changer, gradient shim on any probe, run the selected experiment, and plot the data on any network postscript printer. Need more data, click another button and the **Eclipse+** is off to do your work - and you have not left your office. Contact us at nmr@jeol.com or visit our web site at www.jeol.com.

JEOL USA, Inc., 11 Dearborn Road, Peabody, MA 01960
Tel: 978-535-5900 Fax: 978-536-2205
email: nmr@jeol.com www.jeol.com

JEOL